

**HYDROGEN GENERATION BY  
HYDROLYSIS OF MAGNESIUM AND  
ALUMINIUM ALLOYS AND THEIR  
HYDRIDES**



By

**TSHEPO KGOKANE SEKGOBELA (3984761)**

A thesis submitted in fulfilment of the requirements for the  
degree of

**MAGISTER SCIENTIAE**

In the

**Department of Chemistry**

**Faculty of Science**

**University of the Western Cape, South Africa**

**Supervisor: Dr. Mykhaylo Lototsky**

**Co-supervisor: Dr. Moegamat Wafeeq Davids**

**November 2021**

## ABSTRACT

This study presents the successful characterization and hydrolysis of magnesium hydride ( $\text{MgH}_2$ ) for hydrogen generation. The as-received  $\text{MgH}_2$  served as a precursor in most of the hydrolysis experiments for  $\text{H}_2$  generation. The phase-structural and morphological characteristics of the as-received  $\text{MgH}_2$  were evaluated using scanning electron microscope (SEM), energy dispersive spectroscopy (EDS) and X-ray dispersive diffraction (XRD) characterization techniques. The hydrogen storage performance of the as-received  $\text{MgH}_2$  was analysed by thermogravimetric analysis (TGA), differential scanning calorimetry (DSC) and thermal desorption spectroscopy (TDS) techniques. The hydrolysis of  $\text{MgH}_2$  was performed in a hydrogen generation reactor operated in a batch mode where the temperature and  $\text{H}_2$  flow rate were logged.

The effect of ball milling of  $\text{MgH}_2$  revealed that the reaction kinetics and hydrogen yield for hydrogen generation improved when compared to the as-received  $\text{MgH}_2$ . The ball-milled  $\text{MgH}_2$  hydrogen yield for 2, 4, and 6 hrs milling time was 17.58, 19.74 and 21.09 %, respectively, as compared to 3.35 % for unmilled  $\text{MgH}_2$ .

The influence of organic acids such as acetic acid, citric acid and oxalic acid and their concentration in aqueous solutions on the hydrolysis of magnesium hydride ( $\text{MgH}_2$ ) has been investigated. Different organic acid concentrations of 1, 2, and 3 wt. % was used to study the effect on the hydrolysis of  $\text{MgH}_2$ . The hydrogen generation results indicate that the addition of organic acids to the aqueous solution increases the rate of  $\text{H}_2$  generation as it limits the formation of the  $\text{Mg}(\text{OH})_2$  passivation layer. The increase in the concentration of the organic

acid solutions leads to the increase in the rate and generation of H<sub>2</sub> via hydrolysis of MgH<sub>2</sub>. The addition of organic acids to the reaction solution significantly lowers the activation energy (E<sub>a</sub>) for MgH<sub>2</sub> hydrolysis. The E<sub>a</sub> for MgH<sub>2</sub> hydrolysis in acetic, citric and oxalic acid was 23.53 kJ/mol, 21.62 kJ/mol and 12.70 kJ/mol, respectively, compared to 58.06 kJ/mol in de-ionized water. The organic acid with the fastest hydrogen generation rate is oxalic acid, acetic acid and then citric acid. The pH before and after hydrolysis was recorded and showed that the addition of organic acids suppressed the formation of Mg(OH)<sub>2</sub> passivation layer, causing the aqueous solution to be more acidic, leading to less OH<sup>-</sup> being formed during hydrolysis in the solution.

The effect of AlCl<sub>3</sub> solution with different concentrations of 0.1, 0.2, 0.5 and 1 M was investigated to enhance the hydrolysis of MgH<sub>2</sub>. It was shown that when the concentration of AlCl<sub>3</sub> solution increases, the H<sub>2</sub> yield also increases. The yield for hydrogen generation for 0.1, 0.2, 0.5 and 1 M AlCl<sub>3</sub> solutions were 42.23, 48.92, 74.09 and 96.71 %, respectively.

Finally, the hydrolysis of NaAlH<sub>4</sub> was also investigated as metal alanates have shown to be promising materials for hydrolysis in water for hydrogen generation. The hydrolysis of NaAlH<sub>4</sub> in de-ionized water at 25 °C showed that the reaction is highly exothermic as the reaction temperature increases rapidly and the yield of H<sub>2</sub> was more than 90 % in less than one minute.

## KEYWORDS

Activation Energy

Acetic Acid

Aluminium Alloys

Aluminium Chloride

Ball Milling

Citric Acid

Hydrogen generation

Hydrogen Storage

Hydrolysis

Metal hydrides

Magnesium Hydride

Organic Acids

Oxalic Acid

Reaction kinetics





## LIST OF ABBREVIATIONS

---

ATR	Autothermal Reforming
AWE	Alkaline Water Electrolysis
BM	Ball Milling
COFs	Covalent Organic Frameworks
DSC	Differential scanning calorimetry
EDS	Energy-Dispersive X-Ray Spectroscopy
EHT	Extra High Tension
FEG	Field Emission Gun
GSAS	General Structure Analysis System
LPG	Liquid Petroleum Gas
MEC	Microbial Electrolysis Cells
MOFs	Metal Organic Frameworks
PC	Personal Computer
PEMFC	Proton Exchange Membrane Fuel Cells
PIM	Polymers of Intrinsic Micro-Porosity
PO	Partial Oxidation
SEM	Scanning Electron Microscopy
SOE	Solid Oxide Electrolysis
SMR	Steam Methane Reforming
TDS	Thermal Desorption Studies
TGA	Thermogravimetric Analysis
XRD	X-Ray Diffraction

## DECLARATION

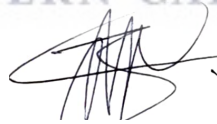
I declare that HYDROGEN GENERATION BY HYDROLYSIS OF MAGNESIUM HYDRIDE AND SODIUM ALANATE is my own work, that it has not been submitted before for any degree or examination in any other university, and that all the sources I have used or quoted have been indicated and acknowledged as complete references.

TSHEPO KGOKANE SEKGOBELA



28 February 2022

UNIVERSITY *of the*  
WESTERN CAPE

A handwritten signature in black ink, appearing to be 'TSHEPO KGOKANE SEKGOBELA'.

Signature -----

# DEDICATION

*This thesis is dedicated to my mother!*



UNIVERSITY *of the*  
WESTERN CAPE

## ACKNOWLEDGEMENTS

Firstly, I would to thank the Lord almighty for the gift of life.

My sincere gratitude to my supervisors Dr. Mykhaylo Lototskyy and Dr. Moegamat Wafeeq Davids for the overwhelming support throughout this journey. This research wouldn't be possible without their kind contribution. Special thanks to my colleagues and friends at South African Institute for Applied Materials Chemistry (SAIAMC) for all the motivation and moral support.

A special thanks to my mother Jane Sekgobela for all the support she has shown me all these years of my life. I would also like to give a special thanks to my brother Paepae Sekgobela for the support. My sister Mareme Sekgobela for offering that kind shoulder to cry on when days were getting too dark.

Special thanks to my friends Tumisho Mabokela for his wise words and moral boosting conversations and Thabang Somo for the seamless car rides that always made sure I'm at the institute on time.

Massive thank you to Dr Remy Bucher at iThemba Labs for the XRD characterization of my samples.

This work has received financial support from South African Department of Science and Innovation (DSI) within Hydrogen South Africa (HySA) Research Development and Innovation Strategy (project KP6-S01 "Metal hydride based hydrogen storage systems"), as well as from the National Research Foundation (NRF) of South Africa (grant numbers 116278 and 132454).

---

## TABLE OF CONTENTS

---

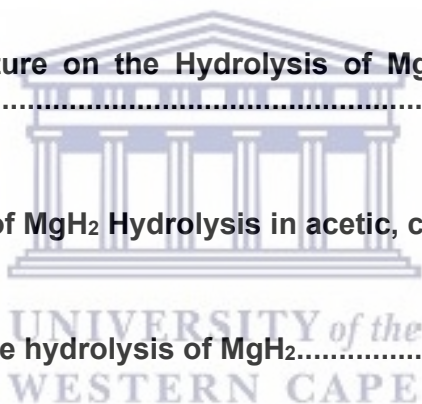
ABSTRACT.....	i
KEYWORDS .....	iii
LIST OF ABBREVIATIONS.....	iv
DECLARATION .....	v
DEDICATION .....	vi
ACKNOWLEDGEMENTS.....	vii
LIST OF FIGURES.....	xii
LIST OF TABLES .....	xv
CHAPTER 1 INTRODUCTION .....	1
1.1 Rationale of the study .....	1
1.2 Problem statement .....	2
1.3 Motivation.....	4



<b>1.4</b>	<b>Aims and objectives .....</b>	<b>5</b>
<b>1.5</b>	<b>Thesis outline .....</b>	<b>6</b>
<b>CHAPTER 2: LITERATURE REVIEW .....</b>		<b>8</b>
<b>2.1</b>	<b>Energy demand and fossil fuels .....</b>	<b>8</b>
<b>2.2</b>	<b>Hydrogen as an energy carrier.....</b>	<b>9</b>
<b>2.3</b>	<b>Hydrogen storage methods.....</b>	<b>13</b>
2.3.1	Compressed Hydrogen.....	14
2.3.2	Cryogenic Liquid Hydrogen .....	15
2.3.3	Physical-Chemical hydrogen storage methods .....	16
<b>2.4</b>	<b>Hydrogen Production.....</b>	<b>16</b>
2.4.1	Hydrogen production from hydrocarbons .....	16
2.4.2	Hydrogen production via electrolysis of water .....	18
2.4.3	Hydrogen production from the reaction of metals with water.....	19
<b>2.5</b>	<b>Magnesium hydride for hydrogen generation.....</b>	<b>21</b>
2.5.1	Hydrogen generation from metal hydrides – Magnesium hydride .....	21
2.5.2	Effects of metal, metal oxide and hydrides on the hydrolysis of MgH <sub>2</sub> .....	22
2.5.3	Effect of halides on hydrolysis of magnesium hydride.....	23
2.5.4	Effect of acids on hydrolysis of magnesium hydride.....	25
<b>2.6</b>	<b>Conclusion of the literature Review.....</b>	<b>26</b>
<b>CHAPTER 3: EXPERIMENTAL METHODOLOGY .....</b>		<b>27</b>

<b>3.1 Chemicals .....</b>	<b>27</b>
<b>3.2 Hydrogen Generation Apparatus .....</b>	<b>28</b>
3.2.1 Hydrogen Reactor Vessel.....	28
3.2.2 Thermostatic water bath .....	29
3.2.3 Moisture Absorbent .....	30
3.2.4 Flow Meters .....	30
3.2.5 pH Meter and Analytical Balance .....	31
3.2.6. Hydrogen generation procedure.....	32
<b>3.3. Planetary Ball Milling .....</b>	<b>33</b>
<b>3.4. Materials Characterization.....</b>	<b>35</b>
3.4.1. Scanning electron microscopy (SEM) & Energy-Dispersive X-Ray Spectroscopy (EDS).....	35
3.4.2 X-Ray Diffraction (XRD).....	36
3.4.3 Thermogravimetric Analysis (TGA) / Differential scanning calorimetry (DSC) .....	38
3.4.4 Sievert Apparatus.....	38
3.4.5. Thermal Desorption Studies (TDS) and re-hydrogenation.....	40
<b>Results and Discussion.....</b>	<b>41</b>
<b>4.1. Characterization of as received MgH<sub>2</sub> .....</b>	<b>41</b>
4.1.1. Scanning electron microscope (SEM) and Energy dispersive X-ray spectroscopy (EDS) of the as-received MgH <sub>2</sub> .....	41
4.1.2. X-Ray diffraction (XRD) analyses of the as-received MgH <sub>2</sub> .....	43
4.1.3. Thermogravimetric analysis (TGA) and Differential scanning calorimetry (DSC) analysis of as-received MgH <sub>2</sub> .....	44
4.1.4. TDS and Re-hydrogenation of Commercial MgH <sub>2</sub> .....	45
4.1.5. Hydrolysis of the as-received MgH <sub>2</sub> at different temperature .....	47

4.1.6. X-ray diffraction (XRD) analyses of ball milled MgH <sub>2</sub> .....	48
4.1.7. Hydrolysis of ball milled MgH <sub>2</sub> .....	51
<b>4.2. Effect of Organic Acid on the Hydrolysis of MgH<sub>2</sub> .....</b>	<b>52</b>
4.2.1. Effect of Acetic acid on hydrogen evolution by Hydrolysis of MgH <sub>2</sub> .....	53
4.2.2. Effect of Citric acid on hydrogen evolution by Hydrolysis of MgH <sub>2</sub> .....	55
4.2.3. Effect of Oxalic acid on hydrogen evolution by Hydrolysis of MgH <sub>2</sub> .....	57
<b>4.3. X-ray diffraction (XRD) analysis of MgH<sub>2</sub> after Hydrolysis in de-ionized water, acetic acid, citric acid and oxalic acid .....</b>	<b>59</b>
<b>4.4. Effect of temperature on the Hydrolysis of MgH<sub>2</sub> in acetic, citric and oxalic acid .....</b>	<b>62</b>
<b>4.5. Activation energy of MgH<sub>2</sub> Hydrolysis in acetic, citric and oxalic acid ..</b>	<b>63</b>
<b>4.6 Effect of AlCl<sub>3</sub> on the hydrolysis of MgH<sub>2</sub>.....</b>	<b>65</b>
<b>4.7. Hydrolysis of Sodium Aluminium Hydride (NaAlH<sub>4</sub>) .....</b>	<b>68</b>
<b>Conclusions and Recommendations .....</b>	<b>70</b>
<b>5.1. Conclusions.....</b>	<b>70</b>
<b>5.2 Recommendation .....</b>	<b>72</b>
<b>REFERENCES.....</b>	<b>73</b>





---

## LIST OF FIGURES

<b><u>Figure</u></b>	<b><u>Description</u></b>	<b><u>Page</u></b>
<b>Figure 3.1:</b>	Five necked flat-bottom flask.....	29
<b>Figure 3.2:</b>	Grant R1 thermostatic water bath.....	29
<b>Figure 3.3:</b>	Moisture trap consisting of CaCl <sub>2</sub> granules.....	30
<b>Figure 3.4:</b>	Two Bronkhorst flow meters 5 and 1 NL for measure amount of hydrogen .....	31
<b>Figure 3.5:</b>	(A) Metrohm 780 pH meter; (B) Kern ACJ 220-4M analytical balance .....	32
<b>Figure 3.6:</b>	Experimental set-up for hydrogen generation via hydrolysis .....	33
<b>Figure 3.7:</b>	Schematic showing the movement of the milling vial (grinding bowl) and the rotating disc during milling operations [60]. .....	34
<b>Figure 3.8:</b>	(A) Fritsch ball mill, (B) Stainless steel vial and (C) Stainless steel balls.....	35
<b>Figure 3.9:</b>	Schematic diagram of Sievert apparatus installation at SAIAMC .....	39
<b>Figure 4.1:</b>	SEM images of the as-received MgH <sub>2</sub> .....	42
<b>Figure 4.2:</b>	(A) EDS spectra of as –received MgH <sub>2</sub> , (B) area of the EDS.....	42
<b>Figure 4.3:</b>	XRD pattern for the as-received MgH <sub>2</sub> .....	43
<b>Figure 4.4:</b>	TGA and DSC analysis of as-received MgH <sub>2</sub> .....	44

**Figure 4.5:** (A) TDS of commercial MgH<sub>2</sub> (1) 1st TDS and (2) 2nd TDS, (B) re-hydrogenation of commercial MgH<sub>2</sub> (1) 1st re-hydrogenation and (2) 2nd re-hydrogenation. .... 46

**Figure 4.6:** Effect of temperature on the Hydrolysis of MgH<sub>2</sub>, (1) 25 °C, (2) 50 °C, (3) 75 °C..... 47

**Figure 4.7:** XRD patterns of as-received MgH<sub>2</sub> and MgH<sub>2</sub> ball milled in H<sub>2</sub> for different times. Peak labels: 1 – α-MgH<sub>2</sub>, 2 – Mg, 3 – γ-MgH<sub>2</sub>, 4 – MgO. Intensities (Y-axis) are shown in arbitrary units (same for all the patterns). ... 49

**Figure 4.8:** Hydrogen generation of ball milled MgH<sub>2</sub> (1) as-received MgH<sub>2</sub>, (2) 2 hrs ball milled MgH<sub>2</sub>, (3) 4 hrs ball milled MgH<sub>2</sub>, (4) 6 hrs ball milled MgH<sub>2</sub> .. 51

**Figure 4.9:** The effect of acetic acid concentration on H<sub>2</sub> generation of MgH<sub>2</sub>, (1) hydrolysis of MgH<sub>2</sub> in de-ionized water, (2) hydrolysis of MgH<sub>2</sub> in 1wt. % acetic acid solution, (3) hydrolysis of MgH<sub>2</sub> in 2 wt. % acetic acid solution, (4) hydrolysis of MgH<sub>2</sub> in 3 wt. % acetic acid solution, (5) hydrolysis of MgH<sub>2</sub> in 4 wt. % acetic acid solution, (6) hydrolysis of MgH<sub>2</sub> in 5 wt. % acetic acid solution..... 54

**Figure 4.10:** The effect of citric acid concentration on H<sub>2</sub> generation of MgH<sub>2</sub>, (1) hydrolysis of MgH<sub>2</sub> in de-ionized water, (2) hydrolysis of MgH<sub>2</sub> in 1wt. % citric acid solution, (3) hydrolysis of MgH<sub>2</sub> in 2 wt. % citric acid solution, (4) hydrolysis of MgH<sub>2</sub> in 3 wt. % citric acid solution, (5) hydrolysis of MgH<sub>2</sub> in 4 wt. % citric acid solution, (6) hydrolysis of MgH<sub>2</sub> in 5 wt. % citric acid solution. .... 56

**Figure 4.11:** The effect of oxalic acid concentration on H<sub>2</sub> generation of MgH<sub>2</sub>, (1) hydrolysis of MgH<sub>2</sub> in de-ionized water, (2) hydrolysis of MgH<sub>2</sub> in 1wt. % oxalic acid solution, (3) hydrolysis of MgH<sub>2</sub> in 2 wt. % oxalic acid solution, (4)

hydrolysis of MgH <sub>2</sub> in 3 wt. % oxalic acid solution, (5) hydrolysis of MgH <sub>2</sub> in 4 wt. % oxalic acid solution, (6) hydrolysis of MgH <sub>2</sub> in 5 wt. % oxalic acid solution.....	58
<b>Figure 4.12:</b> XRD patterns of the deposit after Hydrolysis of MgH <sub>2</sub> in de-ionized water (H <sub>2</sub> O) and 1 wt.% aqueous solutions of acetic (AA), citric (CA) and oxalic (OA) acid. Peak labels: 1 – α-MgH <sub>2</sub> , 2 – Mg, 3 – Mg(OH) <sub>2</sub> . Intensities (Y-axis) are shown in arbitrary units (same for all the patterns). .....	60
<b>Figure 4.13:</b> The hydrolysis of MgH <sub>2</sub> (A) 1wt.% acetic acid at 25, 50 and 75 °C, (B) 1wt.% citric acid at 25, 50 and 75 °C, (C) 1wt.% oxalic acid at 25, 50 and 75 °C .....	63
<b>Figure 4.14:</b> Arrhenius plots for the activation energy for the hydrogen generation in the Hydrolysis of MgH <sub>2</sub> (A) MgH <sub>2</sub> hydrolysis in 1 wt. % acetic acid solution, (B) MgH <sub>2</sub> Hydrolysis in 1 wt. % citric acid solution, (c) MgH <sub>2</sub> hydrolysis in 1 wt. % oxalic acid solution.....	65
<b>Figure 4.15:</b> hydrolysis of MgH <sub>2</sub> in AlCl <sub>3</sub> solutions (1) 0.1 M AlCl <sub>3</sub> solution, (2) 0.2 M AlCl <sub>3</sub> solution, (3) 0.5 M AlCl <sub>3</sub> solution, and (4) 1 M AlCl <sub>3</sub> solution.....	67
<b>Figure 4.16:</b> Hydrolysis of NaAlH <sub>4</sub> in water at 25 °C, (A) reaction solution temperature and H <sub>2</sub> flow rate during hydrolysis, (B) kinetics of H <sub>2</sub> generation. ....	69

## LIST OF TABLES

<u>Table</u>	<u>Description</u>	<u>Page</u>
<b>Table 2.1</b>	– Properties of Hydrogen [2] .....	10
<b>Table 2.2</b>	– Volumetric and gravimetric energy densities of common fuels [20]... ..	12
<b>Table 3.1:</b>	List of Chemicals.....	27
<b>Table 4.1:</b>	Elemental composition of as – received MgH <sub>2</sub> .....	43
<b>Table 4.2:</b>	Results of Rietveld refinement of the studied samples .....	50
<b>Table 4.3:</b>	Reference data for the phases identified during Rietveld refinement of the XRD patterns.....	50
<b>Table 4.4:</b>	pH of acetic acid solutions at different concentrations before and after Hydrolysis of MgH <sub>2</sub> at 25°C.....	54
<b>Table 4.5:</b>	pH of citric acid solutions at different concentrations before and after Hydrolysis of MgH <sub>2</sub> at 25°C.....	56
<b>Table 4.6:</b>	pH of oxalic acid solutions at different concentrations before and after Hydrolysis of MgH <sub>2</sub> at 25°C.....	58
<b>Table 4.7:</b>	Results of Rietveld refinement of the studied samples .....	61
<b>Table 4.8:</b>	pH of AlCl <sub>3</sub> solutions at different concentrations before and after hydrolysis of MgH <sub>2</sub> at 25°C .....	67
<b>Table 4.9:</b>	pH of reaction solution for NaAlH <sub>4</sub> before and after hydrolysis .....	69

# CHAPTER 1 INTRODUCTION

---

## 1.1 Rationale of the study

The rise of atmospheric gas emissions and increasing industrialization forces has led to the scientific research world to find alternatives for reliable, sustainable and renewable clean energy sources. A “sustainable energy source” is one that does not bring about greenhouse emissions and is environmentally friendly and it is not considerably depleted by ongoing use. Currently, the most used primary energy sources include nuclear, oil, coal, and natural gas, all producing greenhouse gases (mainly CO<sub>2</sub>) when combusted and are the leading cause of global warming [1]. Global warming results in climate change, which results in animal species going extinct, icebergs melting, and rising sea level, which endangers the people and organisms living in the low sea-level areas.

The world’s energy resources are limited in quantity. It is only a matter of time until they are depleted, resulting in increasing prices of oil, natural gas, and other fossil fuels. Almost 85% of the world’s primary energy supply is fossil fuel based (oil, natural gas and coal), including 66% of electricity generation leading to production of CO<sub>2</sub> emissions (almost 100%) [2]. Populations living in underdeveloped countries face the cost of unaffordable energy. Carbon dioxide (CO<sub>2</sub>) and nitrous oxide (NO<sub>x</sub>) are released into the atmosphere by some of the

main energy-generating methods and are contributing to environmental pollution [3]. Considerable efforts need to be made to ensure access to affordable, reliable, sustainable, and modern clean energy.

One of the potential alternatives to fossil fuels is hydrogen due to it being readily available, does not produce harmful emissions, is environmentally friendly, fuel-efficient, and is renewable. One of the main obstacles to the implementation of hydrogen as an alternative fuel is hydrogen production. Hydrogen production has been researched over the years due to its attractive advantages as an energy carrier. Hydrogen can be produced mainly from fossil fuel reforming [4], biological hydrogen production [5] and water electrolysis [6]. However, these processes need a lot of energy consumption and expensive catalyst. Hydrogen production via hydrolysis of metals or their hydrides attracts more and more attention mainly due to their high theoretical hydrogen yield, low cost and operating characteristics. Convenient ways of producing hydrogen would significantly boost the fuel cell industry as it is an emerging technology and its success as one of the most efficient energy generators is hanging in the balance [7] if no effective hydrogen production method is developed .

## **1.2 Problem statement**

The main hindrances against the widespread use of hydrogen as an energy carrier are effective hydrogen production methods. It is necessary to produce hydrogen in a manner, which is less energy-intensive, cost-effective and environmentally friendly. Chemical and metal hydrides exhibit an impressive

volumetric hydrogen storage density on a materials basis and therefore, they are promising materials for hydrogen generation. The production of hydrogen via metals or their hydrides holds considerable promise for meeting the hydrogen economy targets. Research on alkali metal borohydrides,  $MBH_4$ , where M is Li, Na, or K has been broad. Although  $NaBH_4$  is the least expensive metal borohydride among these, it suffers from significant setbacks. The high hydrogen storage capacity of sodium borohydride ( $NaBH_4$ ), (about 10.8 wt.%) [8], [9], and moderate operation temperature makes it favourable for hydrolysis. It has been shown that  $NaBH_4$  hydrolysis needs excess water to solubilize the stubborn by-product formed and added base that causes large heat of reaction which makes the fuel regeneration energy-intensive [7].

Most metal hydrides have advantages of gravimetric and volumetric capacities, such as in lithium borohydride ( $LiBH_4$ ) which has 18.5 wt.% and 121  $kg\ m^{-3}$  capacities of hydrogen, respectively. Its theoretical hydrogen capacity of hydrolysis is 13.9 wt.%. Even though  $LiBH_4$  has a theoretical hydrogen capacity higher than most metal hydrides, its practical application is greatly hindered by kinetic and thermodynamic limitations caused by strong covalent and ionic bonds [10]. Although many metal hydrides have been studied and show potential, they suffer major setbacks such as high operational temperatures, toxicity and high costs due to the use of expensive catalysts. [3]

Hydrolysis reaction of  $MgH_2$  produces environmentally friendly residual magnesium hydroxide  $Mg(OH)_2$ . However, this reaction is rapidly interrupted by forming a passive  $Mg(OH)_2$  layer that restricts the direct contact between metal

hydride and water. When  $MgH_2$  is to be used for the generation of hydrogen, a rapid reaction is desired. To accelerate the hydrolysis of  $MgH_2$ , it has been shown by using nanocrystalline  $MgH_2$ , carrying out the process in acidic medium, alloying with other metals, the addition of chlorides, ball milling, the addition of graphite as well as ultra-sonication can improve the efficiency of  $MgH_2$  hydrolysis.

### 1.3 Motivation

Mg has attracted enormous attention over the past years and has been of primary focus in research. This is mainly due to its ability to act as an indirect hydrogen storage material and its low cost and low density. Also, hydrogen generation from  $MgH_2$  is a renewable and environmentally friendly process. The high hydrogen release from the Mg-water reaction reaches the hydrogen evolution of about 933 mL/g, and its hydrogen storage value reaches up to 7.6 weight % [10].

Hydrogen production by hydrolysis of metal hydrides has lured attention from researchers due to their high energy density by volume and safety. Magnesium hydride ( $MgH_2$ ) has the highest energy density among the reversible metal hydrides, which is at about (9MJ/Kg Mg). During hydrolysis reactions, chemical hydride reacts with water to produce hydrogen. Another advantage of  $MgH_2$  is that it offers thermal stability, high density and ease of high purity release of hydrogen stored in the metal hydride [11].



The hydrolysis of  $\text{MgH}_2$  is a potential method of generating hydrogen, as  $\text{MgH}_2$  is non-toxic and inexpensive compared to other hydrolysis agents. In a closed cycle,  $\text{MgH}_2$  has the potential to be generated industrially with a moderately high overall energy efficiency. Additionally, it is thermodynamically stable in the absence of moisture and therefore has a long-life span. To improve the efficiency of the hydrolysis of  $\text{MgH}_2$ , one has to limit the production of the  $\text{Mg}(\text{OH})_2$  passive layer during hydrolysis reaction; organic acids have been shown to limit the passive layer production. They are also environmentally friendly and very inexpensive and help improve the reaction rate and kinetics of hydrolysis reactions [12].



#### 1.4 Aims and objectives

This research project is aimed at the identification of materials based on lightweight metals, alloys and hydrides as candidates for  $\text{H}_2$  generation. The focus will be on  $\text{MgH}_2$  as a potentially inexpensive material, which undergoes hydrolysis in a neutral or slightly acidic medium, most compatible with operating conditions of proton exchange membrane fuel cells (PEMFC) used in the target applications.

The project sub-goals include:

- The main objective of this research is to find the most effective method to produce the maximum yield of hydrogen from the hydrolysis of  $\text{MgH}_2$ . The hydrolysis of  $\text{MgH}_2$  depends on the structure of the  $\text{MgH}_2$ , which are controlled by parameters such as ball milling, type of additives and the amount of additives.

- To determine the effect of ball milling time on the  $\text{MgH}_2$  for hydrogen generation by hydrolysis
- To determine the influence of different organic acids on the hydrolysis of  $\text{MgH}_2$  for hydrogen generation.
- To determine the effect of chlorides ( $\text{AlCl}_3$  and  $\text{MgCl}_2$ ) on the hydrolysis of  $\text{MgH}_2$  for hydrogen generation.
- To ball mill  $\text{NaAlH}_4$  with  $\text{MgH}_2$  and study the effect it has on hydrolysis reaction.

### 1.5 Thesis outline

- Chapter one gives a general introduction to the research study. It details the aims and objectives of the projects and details the problem statement and motivation for the study.
- Chapter two gives a review of various studies related to the topic. A review on various hydrogen storage methods such as compressed  $\text{H}_2$  storage, cryogenic liquid  $\text{H}_2$  storage and physical-chemical  $\text{H}_2$  storage methods, and a review on hydrogen generation technologies such as  $\text{H}_2$  generation from hydrocarbons,  $\text{H}_2$  generation from electrolysis and  $\text{H}_2$  generation from the reaction of metals with water. In this chapter, a review on magnesium hydride for hydrolysis application was also focused on.
- Chapter three provides a detailed account of the materials, experimental methods, research design and equipment used in the study. A description

of all the characterization techniques is discussed, such as SEM, EDS, XRD, TGA, DSC and TDS.

- Chapter 4 contains results and discussions of major findings on the material characterization carried out on the reaction substrates. The chapter discusses various experimental investigations on the hydrolysis of  $\text{MgH}_2$ , such as the effect of temperature and ball milling. The chapter also discusses the role of organic acids and aluminium chloride in the hydrolysis of  $\text{MgH}_2$ . Furthermore, a discussion on  $\text{NaAlH}_4$  as a promising material for hydrolysis was elaborated on.
- Chapter 5 summarizes the objective achieved pertaining to the study. The chapter ends with recommendations for future studies.



---

## LITERATURE REVIEW

---

### 2.1 Energy demand and fossil fuels

It is well known that the world's energy resources are depleting, and they will inevitably run out in the future. This is due to the ever-increasing world's population and industrialization. A report in 2018 suggested that non-renewable resources are responsible for 85% of total energy consumption worldwide [13]. Environmental issues (global warming) and economic issues arise from the use of resources such as coal, natural gas and oil. In order to achieve a sustainable energy future, the challenges that arise with the depletion of limited fossil fuels need to be overcome [14].

It was suggested in numerous 2015 studies that natural gas, coal and oil reserves are expected to last for approximately 200, 40 and 60 years, respectively, if consumption continues at the current rate. Peak production rates of liquid fuels and natural gas occurred between 2005 and 2015 and the same trend is predicted to repeat again in 2030; the occurrence seems likely to occur. The advancement in human intelligence may have been attributed to the discovery and utilization of these reserves. Although the reserves are limited, more discoveries are still increasing to date [15]. Hook et al. reported that fossil fuels such as natural gas (20.9%), oil (32.8%) and coal (27.2%) account for more than 80% of the world's primary energy resources [16].

Buildings and infrastructure increased the global fossil fuel expenditure by 36% between 1971 and 2010 (including natural gas, coal and oil) [17]. The impacts of climate change, which is still on the rise, is still the greatest challenge of the twenty-first century, it may still be avoided if valid strides are made to change current energy systems. Greenhouse gases and emissions from fossil fuel-based power generating can be displaced by renewable energy sources that can eliminate climate change [18].

Growth by 2.3% between 2012 and 2013 on per capita energy consumption populations increase was recorded, resulting in global energy consumption rates to continue rising. Industrialised nations have decreased their human population and this may be a result of strong policies on family planning, but higher per capita energy consumption may be attributed to increased wealth driving this trend [19].

## **2.2 Hydrogen as an energy carrier**

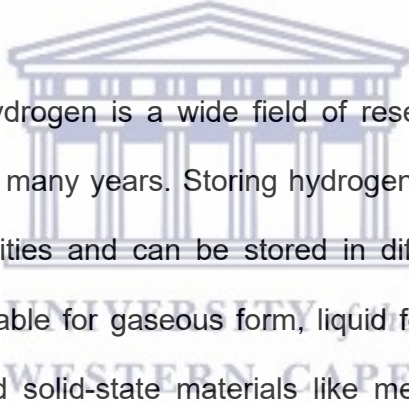
Hydrogen is the most abundant element in the whole universe, owing to it being the lightest in molecular structure, smallest and simplest of all elements. It is a colourless, odourless and tasteless element. It is found primarily in combination with other elements but separated from these elements; it becomes an attractive fuel for energy. Energy is generated when it is burned or combined with oxygen, such as in fuel cells, producing only water as a by-product. It is found in nature, primarily occurring in water with oxygen, fossil fuels, and living organisms with nitrogen and carbon [20].

Hydrogen exists in three isotopes: protium, deuterium and tritium. Protium, which is the simplest one, is the main constituent of hydrogen and consists of one proton and one electron. Among all fuels, hydrogen has the highest energy content per unit mass, even though it is the lightest element. The energy required for the production of hydrogen is always greater than the energy output from hydrogen. This will mean that, for hydrogen to be produced, a feedstock and energy will be required. The expansion of renewable resources will come in handy in eradicating present fossil fuel dependence if we take into consideration the increasing rates of energy consumption in the world and its adverse effects [2].

**Table 2.1** – Properties of Hydrogen [2]

Molecular weight	2.016	Amu
Density		
Gas	0.0838	Kg/m <sup>3</sup>
Liquid	70.8	Kg/m <sup>3</sup>
Temperature (Boiling)	20.3	K
Critical point		
Temperature	39.94	K
Pressure	1284	kN/m <sup>2</sup>
Density	31.40	kg/m <sup>3</sup>
Temperature (Self-ignition)	858	K
Ignition limits in air	4-75	(vol %)
Stoichiometric mixture in air	29.53	(vol %)

Hydrogen is a state-of-the-art energy carrier, which can be used without any emissions at high efficiency. When hydrogen is being used to generate electricity in fuel cells or when combusted with air, only water and a small quantity of NO<sub>x</sub> are products. Although most of the hydrogen research is still on a small to medium scale, it has been technically proven that hydrogen can replace current fossil fuels in many ways that they are used. Be it for heating, power generation or transportation. The attractive electrochemical properties of hydrogen are attracting use in fuel cells. Hydrogen is environmentally friendly and regenerative and exhibits the highest heating value per mass among all fuels.



The storage of hydrogen is a wide field of research on its own and has attracted researchers for many years. Storing hydrogen plays a considerable role in its application capabilities and can be stored in different forms. Large scale hydrogen storage is suitable for gaseous form, liquid form is suitable for air and space transportation and solid-state materials like metal hydrides are ideal for stationery application storage requirements. Hydrogen has a wide variety of attractive features on the economy, including (i) its renewable and sustainable energy, (ii) decreased pollution and better urban air quality and (iii) reduces dependence on oil imports [14].

**Table 2.2** – Volumetric and gravimetric energy densities of common fuels [20].

Material	Energy per kilogram (MJkg <sup>-1</sup> )	Energy per liter (MJl <sup>-1</sup> )
Hydrogen (liquid)	143	10.1
Hydrogen (compressed, 700 bar)	143	5.6
Hydrogen (ambient pressure)	143	0.0107
Methane (ambient pressure)	55.6	0.0378
Natural gas (liquid)	53.6	22.2
Natural gas (compressed, 250 bar)	53.6	9
Natural gas	53.6	0.0364
LPG propane	49.6	25.3
LPG butane	49.1	27.7
Gasoline (Petrol)	46.4	34.2
Biodiesel oil	42.2	33
Diesel	45.4	34.6

The storage densities for hydrogen are not greater than those for gasoline storages on both mass and volume bases. Liquid hydrogen storages provide the highest energy storage densities on a mass basis, approximately 20% less than gasoline storage density. Metal hydride storage, whose energy density is approximately 35 % that of gasoline storage, provides the highest hydrogen energy storage density on a volume basis. Generally, as reported in 2013, gasoline has the highest storage density on both a mass and volume basis and no hydrogen storage option has high energy. This issue arises in applications of hydrogen as a fuel in fuel cell vehicles [21].



Hydrogen has an energy density of  $143 \text{ MJ kg}^{-1}$ , a figure that is up to three times that of liquid hydrocarbon-based fuels. Highly debatable remains the use of hydrogen as the power carrier in various sectors to reduce harmful gas emissions. At the moment, however, it is not cost-effective [22]. Depending on the level of demand, availability of resources, regional factors and progress on hydrogen technology, many solutions for hydrogen supply are likely to emerge. The focus should be on hydrogen utilization in large cities with air pollution problems or limited nations with high imported fuel costs should develop [23].

### 2.3 Hydrogen storage methods

Many researchers have considered hydrogen as the best sustainable primary energy for the future. Hydrogen is a crucial technology for the sustainable development of hydrogen power, which is essential for future economic prosperity [24].

The use of hydrogen as an alternative fuel for the future depends on its proper distribution and storage. Safety is important in hydrogen storage systems and should be included together with high volumetric and gravimetric efficiency when selecting a storage method. There are two main types of hydrogen storage methods namely, physical methods and physical-chemical methods. In physical methods, hydrogen gas is compacted in a storage medium with no interaction between the storage medium and hydrogen molecules. In physical-chemical, there is an interaction of molecular or atomic hydrogen with the storage medium [25]. Various methods and technologies of hydrogen storage are considered in numerous review articles: above 800 Scopus-indexed documents which contain

phrases “hydrogen storage” and “review” were published in the period 2015–2021. Several important reviews [26-30] analysing physical and physical-chemical (materials-based) hydrogen storage technologies are typical representatives of these studies. Below, we briefly consider two physical hydrogen storage methods (compressed and cryogenic liquid hydrogen) and give a brief outlook of several physical-chemical hydrogen storage methods.

### 2.3.1 Compressed Hydrogen

The standard method for H<sub>2</sub> storage is to compress gaseous hydrogen with a peak operating pressure of 20 MPa in high-pressure gas cylinders. Current applications for fuel cells currently require pressurisation of hydrogen between 35 MPa and 70 MPa. Compressed hydrogen is a matured technique for the storage of hydrogen and the energy density owing to the volumetric increase with the gas pressure [31].

Hydrogen storage characteristics are improved by reducing the cylinder weight by using lighter materials and increasing the working pressure. Advantages of compressed gas storage methods are that they are reliable, storage time is infinite and easy to use and affordable. Its main disadvantage is the dependency on storage pressure, which causes the low storage density—high-pressure storage results in higher capital and operating costs.

Hydrogen storage in compact and lightweight high-pressure cylinders is still a challenge since these cylinders have a high capital cost and safety concerns.

### 2.3.2 Cryogenic Liquid Hydrogen

The most attractive traits of liquefied hydrogen are its high liquid density and storage efficiency. Cryogenic tanks are mostly used for storing liquid hydrogen (253 °C) at ambient pressure. To avoid hydrogen pervading the storage walls, material resistant to embrittlement are very significant. Although aluminum tanks are common for vehicle applications, double-wall cylindrical stainless are an alternative.

Transportation of large amounts of hydrogen require these kinds of storage method for industrial applications. Cryogenic liquid hydrogen suffers from several drawbacks that hinder its widespread use.

As less as 15.1 MJ/kg [32] of energy is required for the liquefaction process thus reducing the overall efficiency of a system responsible for liquid hydrogen storage. Heat leaks may lead to 'boil off' losses within the system - the rate of which depends on the size and shape of the vessel.

Air and space applications are most suitable for Liquid hydrogen storage because such applications are not dependent on the cost of hydrogen and it is used in short periods of time.

### 2.3.3 Physical-Chemical hydrogen storage methods

This method relies mainly on the chemical sorption where hydrogen is split into atoms and combined with the chemical structure of the storage material and physical sorption where hydrogen is stored in porous materials. The most sought-after group of materials associated with chemical sorption are metal hydrides. Hydrogen is chemically bonded in the metal hydrides.

Carbon-based materials such as activated carbon, zeolites, fibres, carbon nanotubes, covalent organic frameworks (COFs), metal-organic frameworks (MOFs) and polymers of intrinsic micro-porosity (PIMs) employ van der Waals interactions to adsorb molecular hydrogen on surfaces of solids. Porous carbon materials and Metal-Organic Frameworks (MOFs) among all are known to be the most promising. Significant hydrogen storage densities are achieved by high pressure and low temperatures during adsorption due to the bonding weakness of the van der Waals forces. Different techniques can be employed to liberate the hydrogen stored whenever required, sometimes by thermal stimulation.

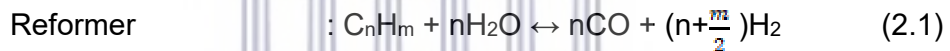
## 2.4 Hydrogen Production

### 2.4.1 Hydrogen production from hydrocarbons

Hydrogen can be obtained from hydrocarbons (mainly from natural gas) by several chemical methods. Among these methods, Steam Methane ( $\text{CH}_4$ ) Reforming (SMR), producing approximately 74% hydrogen yield efficiency, is the most widely used. SMR technology is boasts advantages of being least expensive and cost effective due to its feedstock being both liquid and gaseous

hydrocarbons. Other methods include Auto thermal reforming (ATR) and partial oxidation (PO<sub>x</sub>). [33], [34] [14], [35].

In steam reforming, Hydrogen and carbon monoxide (CO) are produced by mixing natural gas that is cleaned of impurities with steam in heat reactor. This is followed by the conversion of CO and water to hydrogen and carbon dioxide in the catalytic water gas shift reaction. Metal such as nickel (non-precious metal), platinum or rhodium (precious metals) are typically used as catalysts for the reforming reaction. The main SMR chemical reactions are as follows: [2], [36]



However, the main drawback of this approach is that the hydrogen produced suffers from high pollution and limited resources. The carbon monoxide and carbon dioxide produced from this method are known as greenhouse gases and are not environmentally friendly. This method is not recognized as “green” because the resources are non-renewable.

The second most used method for hydrogen generation is partial oxidation. In this the process the generation is achieved through the conversion of oxygen, steam and hydrocarbon. Natural gas or hydrocarbon is introduced into a reformer where it is heated in the presence of a limited amount of pure oxygen. In this

process, temperatures are elevated to 1200-1350°C to react oxygen with hydrocarbon fuel in a lower than normal stoichiometric ratio, yielding a mixture of hydrogen and carbon monoxide [37], [38].

In Auto thermal reforming, Steam Methane Reforming and Partial Oxidation are combined. Partial oxidation is used to produce heat and steam reforming to increase hydrogen production. Natural gas is first oxidized into syngas ( $\text{CO} + \text{H}_2$ ) in a catalytic furnace and then  $\text{CO}$  reacts in the presence of water to form  $\text{CO}_2$  and  $\text{H}_2$  by a catalytic shift reaction.  $\text{CO}_2$  formed at the end is captured by amines through an absorption process [39].

#### **2.4.2 Hydrogen production via electrolysis of water**

Electrolysis produces high purity of hydrogen (99.999%) and eco-friendly by splitting water to give out pure hydrogen and water. The production of hydrogen via water splitting is promising, especially if renewable energy is used as an energy source, which leads to only pure oxygen as a by-product.

One of the electrolysis methods which has attracted the most attention researchers is the PEM water electrolysis due to its environmental impact and sustainability. The others are Solid oxide electrolysis (SOE), Alkaline water electrolysis (AWE) and Microbial electrolysis cells (MEC). The compact design of PEM water electrolysis makes it to be one of the most favourable methods for conversion of renewable energy to high purity hydrogen. Other promising attributes are high current density (above  $2 \text{ A cm}^{-2}$ ), high efficiency, fast response,

small footprint, operates under lower temperatures (20–80 °C) and produced ultrapure hydrogen and also produced oxygen as a by-product [40 - 43].

However, hydrogen production efficiency through PEM water electrolysis is still low to be economically competitive due to the high energy consumption and low hydrogen evolution rate.

### 2.4.3 Hydrogen production from the reaction of metals with water

Hydrogen production by the reaction of certain metals with water has been studied by researchers for many years. The group IA and IIA of the periodic table form corresponding metal hydroxide and hydrogen when they encounter water. One of the most extensively researched metal for hydrolysis is aluminium. Aluminium is a good choice for hydrolysing metal since it is abundant and light [44]. The challenge with the aluminium-water reaction is the oxide layer of aluminium that forms on the surface of aluminium particles and consequently inhibits the water from directly getting into contact with the aluminium metal. The reaction between aluminium and water is as follows:



The gravimetric hydrogen capacity from this reaction is 3.7 wt.% and the volumetric hydrogen capacity is 46 g H<sub>2</sub>/L [45]. Researchers have focused on removing the oxide layer, and one of the common methods used is placing aluminium in alkaline environments. The use of hydroxides such as NaOH and

KOH has been found to remove the oxide layer; however, one of the challenges with using alkaline solutions is the corrosion of the apparatus [46]. The reaction can also go ahead by adding special additives to the aluminium in small quantities [47]. Aluminium alloys with different metals such as Ga, In, Zn, Sn and Bi have been suggested. One study by Elitzur et al. mixed Al alloys with various metals and even though the water was in contact with the Aluminium surface, the reaction occurred at elevated temperatures. This resulted in a slow reaction rate with water due to the slow melting of the alloys [48]. Al and Al-based alloys are promising for hydrolysis reaction because they can generate a large amount of theoretical hydrogen; however, the strong affinity of Al with oxygen interrupts the self-corrosion process, leading to its sluggish hydrogen-generating rate.

Sodium borohydride ( $\text{NaBH}_4$ ) has also been shown to be a promising chemical hydride for hydrolysis reaction due to its high hydrogen storage capacity of 10.8% and moderate operation temperature for hydrolysis [49]. The hydrolysis of  $\text{NaBH}_4$  produces pure hydrogen gas, with the ideal stoichiometry shown in the equation below.



Researchers have focused on various catalysts to increase the reaction kinetics of hydrogen production from the hydrolysis of  $\text{NaBH}_4$ . Sahin et.al reported on the hydrolysis of  $\text{NaBH}_4$  in a reaction catalyzed with Pd. It was reported that the use of Pd catalyst enhanced the reaction kinetics resulting in improved hydrogen generation [50]. It was also reported by Amendola et al. the use of Ru as a catalyst



for hydrolysis of  $\text{NaBH}_4$ . They reported higher and more sustainable hydrogen production in alkaline conditions ( $\text{pH} > 11$ ) for the adequate acceleration of the reaction kinetics by ruthenium (Ru) catalyst in an on-demand hydrogen reactor [51]. However, the relatively high cost and the complicated regeneration process of  $\text{NaBH}_4$  and the by-product sodium metaborate, which is a corrosive material, limits their application in hydrogen generation via hydrolysis.

## 2.5 Magnesium hydride for hydrogen generation

### 2.5.1 Hydrogen generation from metal hydrides – Magnesium hydride

One of the most exciting metal hydrides is magnesium hydride ( $\text{MgH}_2$ ) due to its attractive features. Magnesium hydride has a hydrogen capacity of 7.6 wt.% and a relatively low production cost [52].  $\text{MgH}_2$  is a promising material because it is cheap and non-toxic contrary to other hydrolysis hydrides like  $\text{NaBH}_4$  and  $\text{LiBH}_4$ . It has a high hydrogen storage capacity of up to 15.3 wt. % (if the water is included to the calculation) and a long shelf life due to its thermodynamic stability in the absence of moisture

It is also important to note the abundance of Mg on earth. The instability of  $\text{MgH}_2$  when in contact with water is a favourable advantage for hydrolysis. The hydrogen capacity of  $\text{MgH}_2$  decreases to 6.4wt% when water is excluded [11]. This method of hydrogen production faces considerable challenges. The hydrolysis of  $\text{MgH}_2$  and other similar reactions suffer from slow reaction kinetics and exercising high purity hydrogen output. The slow kinetics come as a result of the formation of a dense passive layer of  $\text{Mg(OH)}_2$  on the surface when water gets into contact with

MgH<sub>2</sub> [53]. The hydrolysis of Mg and MgH<sub>2</sub> can be described by the following reactions:



Many methods have been researched to overcome this problem and the research is still ongoing. The most studied are the use of catalysts to accelerate the reaction kinetics, ball milling and the use of acids. Some researchers use both methods on the same reaction. One study by Hiraki et al. used a weak acid such as citric acid to determine its effect on the hydrolysis of MgH<sub>2</sub>. He used different concentrations and only distilled water for hydrogen production.

Ma et al. studied the use of low energy ball milling and metal halides as catalysts to obtain high yields of hydrogen. The study also included metal salts that undergo hydrolysis without any assistance. The study discovered that the addition of metal salts highly increase the reaction kinetics and yield of MgH<sub>2</sub> hydrolysis reaction [11]. Another study that used MgH<sub>2</sub>-LiNH<sub>2</sub> composite found that the hydrolysis properties of MgH<sub>2</sub> were enhanced by introducing LiNH<sub>2</sub> in the ball-milled composites generating up to 1016 mL g<sup>-1</sup>[11].

### 2.5.2 Effects of metal, metal oxide and hydrides on the hydrolysis of MgH<sub>2</sub>

Pure metals and their hydrides additives are widely used as catalysts, which generally affects the reaction to change the hydrolysis pathway. Numerous efforts have been dedicated to improving the kinetics of the hydrolysis reaction through milling Mg or MgH<sub>2</sub> with metallic catalytic agents. Metals such as nickel

and titanium have been studied and some interesting findings have been made. In a study by Huang et al., hydrolysis of  $\text{LaH}_3/\text{MgH}_3$  was greatly enhanced when nickel was added to the reaction to form the  $\text{LaH}_3/\text{MgH}_3/\text{Ni}$  composite [54].

Transition metals are known for their ability to promote the dissociation of hydrogen by destabilizing the Mg-H bonding [55]. Cobalt and nickel are the most used non-noble metals due to their abundance and low cost compared to noble metals. Incorporating  $\text{MgH}_2$  with other hydrides to form composites tends to increase the hydrogen capacity. An example is the  $\text{MgH}_2\text{-LiNH}_2$  which exhibit a hydrogen capacity of 8.1 wt%. Studies show that this composite can generate up to 1016 ml  $\text{g}^{-1}$  of hydrogen. It was proven to be stable in air, which is suitable for hydrolysis applications [11].

$\text{TiH}_2$  and Al additives do not influence the particle size and the number of defects as opposed to  $\text{MgO}$ , and thus generating more hydrogen during hydrolysis of  $\text{MgH}_2$  [56]. Selected doped additives such as  $\text{TiCl}_3$  are found to have higher catalytic activity. In one study by Wang et al., a combination of  $\text{TiCl}_3$  and graphene oxide based porous carbon was used to enhance the hydrogen evolution from hydrolysis of  $\text{MgH}_2$ . This composite improved the hydrolysis significantly [57].

### 2.5.3. Effect of halides on hydrolysis of magnesium hydride

Halides have formed a considerable part of hydrogen generation for some time now. In a study by Sevastyanova and co-workers where  $\text{MgCl}_2$  was compared with  $\text{MgBr}_2$ , it was observed that hydrolysis reactions of  $\text{MgH}_2$  involving

chlorides were faster and more efficient,  $\text{CuCl}_2$  included [58]. Metal halides ammine complexes give off ammonia and  $\text{H}_2$  [59].

It has been shown that some transition metal halides show good catalytic properties. The dehydrogenation kinetics of  $\text{H}_2$  from  $\text{MgH}_2$  is not troubled by the addition of group i and ii halides. Malka et al. conducted a study in which the group iv to v halides of the periodic table were better catalysts than others. This study has also shown that fluorides are better than chlorides [60].

Gan et al. studied the effect of  $\text{AlCl}_3$  solution with different concentrations at various temperatures on the hydrolysis of  $\text{MgH}_2$  and discovered the solution to have enhanced the hydrolysis. Conversion rate reached as high as 90,53% [61].

Berezovets et al [62] have recently studied kinetics and mechanisms of  $\text{MgH}_2$  hydrolysis in  $\text{MgCl}_2$  solutions. It was shown that the increase of  $\text{MgCl}_2$  amount results in the increase of hydrolysis efficiency. The highest hydrogen yield (1025 mL ( $\text{H}_2$ )/g  $\text{MgH}_2$ ) was achieved for the stoichiometric ratio  $\text{MgH}_2+0.7\text{MgCl}_2$  ( $\text{MgCl}_2/\text{MgH}_2 = 12.75/100$  by weight). Analysis of the literature data on the influence of the chloride additives ( $\text{ZnCl}_2$ ,  $\text{AlCl}_3$ ,  $\text{FeCl}_3$ ,  $\text{ZrCl}_4$ ) on hydrolysis of magnesium hydride showed that the conversion rate increases significantly when the pH of the reaction solution decreases from 6.5 to <1. At the same time, the experiments showed that in the case of  $\text{MgCl}_2$  whose solutions exhibit significantly higher values of pH=6–7 the effect of the increase of the conversion rate is much higher. The observed effect was associated with the formation of the buffer solution that controls the pH of the reaction mixture [62].

#### 2.5.4. Effect of acids on hydrolysis of magnesium hydride

The use of acids in the hydrolysis of  $\text{MgH}_2$  has been ongoing research since the 2000s. Acids have been reported to be harmful and toxic to humans. In hydrolysis experiments, it is advisable not to use strong acids as they are not environmentally friendly and can produce vigorous, sometimes uncontrollable reactions. The use of acids has been reported to corrode working equipment. However, it has been argued that it is only the case with strong acids [63].

The hydrolysis of  $\text{MgH}_2$  is abruptly interrupted by a passive hydroxide layer that forms during the reaction. This layer of  $\text{Mg(OH)}_2$  can be broken by the introduction of organic acids [64]. Acetic acid and citric acid have been widely studied and show excellent properties. One study employed the use of citric acid for hydrolysis of  $\text{MgH}_2$  tablets was developed. The conversion yield was as high as 70% [65].

Chloride salts have been found to be of benefit for the hydrolysis kinetics of Mg-based material. Chloride salts are brittle in nature, this fact helps in the milling process by increasing and exposing the specific area of the powder by generating many scrappy particles. Li et al. studied the effects of  $\text{NaCl}$ ,  $\text{MgCl}_2$  and  $\text{NH}_4\text{Cl}$  on hydrogen evolution performance. The best hydrogen production performance was shown by  $\text{MgH}_2$ -10% $\text{NH}_4\text{Cl}$  with a high yield of 1311 ml/g [66].

## 2.6 Conclusion of the literature Review

This summary is based on the literature survey carried out in this chapter. It has to be noted that there is no ideal material for hydrolysis reaction.  $MgH_2$  has been shown to be a promising material for hydrolysis. The attractiveness of  $MgH_2$  for hydrolysis is due to low cost, the abundant raw material (the earth's crust contains 2 wt. %), stability in contact with air and environmentally friendly. Magnesium hydroxide ( $Mg(OH)_2$ ), is the only by product of  $MgH_2$  hydrolysis reaction, which is environmentally friendly. However, the main drawback of  $MgH_2$  for the generation of  $H_2$  is that the hydrolysis reaction is stopped suddenly because of the formation of a passive layer of  $Mg(OH)_2$  bonded on the material surface. To improve the hydrolysis of  $MgH_2$  which was shown to be facilitated by the lowering of pH of the reaction solution, we have recommended approaches aimed at turning the solution composition by the addition of different organic acids.



UNIVERSITY of the  
WESTERN CAPE

---

## EXPERIMENTAL METHODOLOGY

---

This chapter presents information on the various materials used in this study as well as the methodology employed in accomplishing the set objectives. The chapter is divided into three different sections, materials used, hydrogen generation set-up and experimental procedure.

### 3.1 Chemicals

The hydrolysis experiments in this study were all performed with deionized water obtained from a Milli-Q water purification system. All chemicals used for experimental work in the study were of analytical grade. Table 3.1 lists the chemicals used for the experimental work within the research study.

**Table 3.1:** List of Chemicals

Chemical	Supplier
MgH <sub>2</sub> (98%)	Alfa-Aesar
MgCl <sub>2</sub> (99%)	Alfa-Aesar
AlCl <sub>3</sub> (99%)	Alfa-Aesar
CaCl <sub>2</sub> (98%)	UniLab
NaAlH <sub>4</sub> (93%)	Sigma-Aldrich
Citric Acid	Sigma-Aldrich
Oxalic Acid (98%)	AR-Kimix
Acetic Acid	Sigma-Aldrich

## 3.2 Hydrogen Generation Apparatus

This section focuses on the experimental apparatus involved in the hydrogen generation experiments. The experimental set-up for hydrogen generation by hydrolysis was developed and constructed at the South African Institute of Advanced Chemistry (SAIAMC) at the University of the Western Cape (UWC). The hydrogen generation set-up consists of a five necked flat-bottom jacketed flask that serves as the reaction vessel, thermostatic regulated water bath, moisture absorbent unit, flow meters (Bronkhorst 1 and 5 NL/min), and data logger. Figures and images will illustrate different components for the hydrogen generation experiment. The experimental apparatus and settings will be discussed in the following subsections.

### 3.2.1 Hydrogen Reactor Vessel

A 200 ml five necked borosilicate flat-bottom jacket flask was used for hydrogen generation experiments. The five necked flat jacket flask was used due to the fact that the jacket was used to circulate water from the thermostatic bath to regulate the temperature of the hydrolysis experiment. Figure 3.1 shows a picture of the hydrogen reactor vessel used in hydrolysis experiments. Only three necks were used during hydrolysis experiments, while two inlets were sealed. Of the three necks utilized, the left neck of the flask is a passage for hydrogen evolved from the hydrolysis reaction. The middle neck is used to introduce the sample and solvent (acidic solutions and water) before commencing with the experiment. The far-right neck of the flask connects with a thermocouple to monitor the temperature of the reaction.





**Figure 3.1:** Five necked flat-bottom flask

### 3.2.2 Thermostatic water bath

A Grant R1 series thermostatic circulatory water bath was used to regulate the temperature of the reactor vessel during hydrolysis experiments. Figure 3.2 shows a picture of the thermostatic circulatory water bath used. The thermostatic water bath was used to study the effect of different temperatures on the hydrolysis reaction. Hydrolysis experiments were carried out at various temperatures 25, 50 and 75°C, respectively.



**Figure 3.2:** Grant R1 thermostatic water bath

### 3.2.3 Moisture Absorbent

Hydrogen produced via hydrolysis contains small amounts of moisture, which needs to be removed before it passes to the flow meters as it can lead to inaccurate readings and damage the flow meters. A moisture trap was used to absorb most of the moisture, the absorbent used in the moisture trap is calcium chloride ( $\text{CaCl}_2$ ) granules. The moisture trap was made using a  $\frac{1}{2}$  inch plastic Swagelok tube 20 cm long, which was packed with  $\text{CaCl}_2$  granules. Figure 3.3 shows a picture of the moisture trap used in the hydrolysis experiments.



**Figure 3.3:** Moisture trap consisting of  $\text{CaCl}_2$  granules

### 3.2.4 Flow Meters

Flow meters were used to measure the amount of hydrogen generated during the hydrolysis experiments. The principle of the flow meters estimates hydrogen amount based on its thermal conductivity; this is due to different gases having different thermal conductivities. Two Bronkhorst  $\text{H}_2$  flow meters with varying rates of flow 1 and 5 NL were used in the hydrolysis set-up. The reason for using two flow meters is because at the beginning of the hydrolysis experiment, the  $\text{H}_2$  flow rate is high and as the experiment proceeds the flow drops; by employing two flow meters, we can calculate more accurately the amount of hydrogen produced

during the experiment. Figure 3.4 shows a picture of the two flow meters. The Flowmeters are controlled using LabVIEW program.

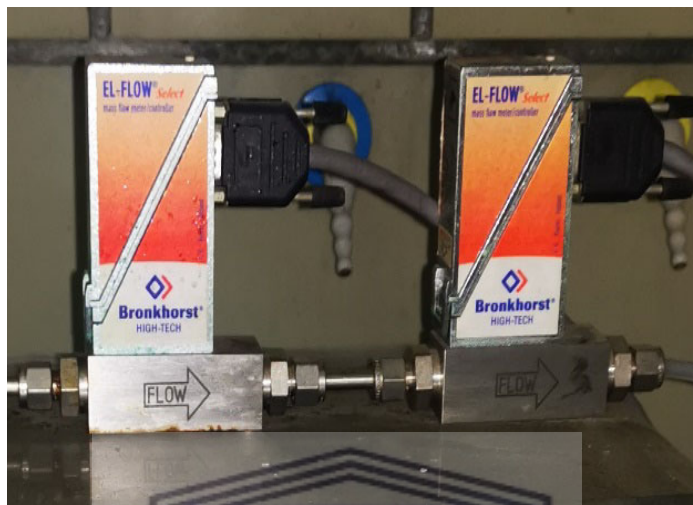


**Figure 3.4:** Two Bronkhorst flow meters 5 and 1 NL for measure amount of hydrogen

### 3.2.5 pH Meter and Analytical Balance

Figure 3.5 (A) shows the 780 pH Meter from Metrohm used to measure the pH of the solution before and after the hydrolysis experiment. The small weight of  $\text{MgH}_2$  (200 mg) used in the hydrolysis experiments was kept constant throughout this study. The accuracy of the weight of all samples was essential for the success of the hydrolysis experiments. The analytical weighing balance is shown in Figure 3.5 (B); the model is an ACJ 220-4M Kern, which has an accuracy of four decimal places.

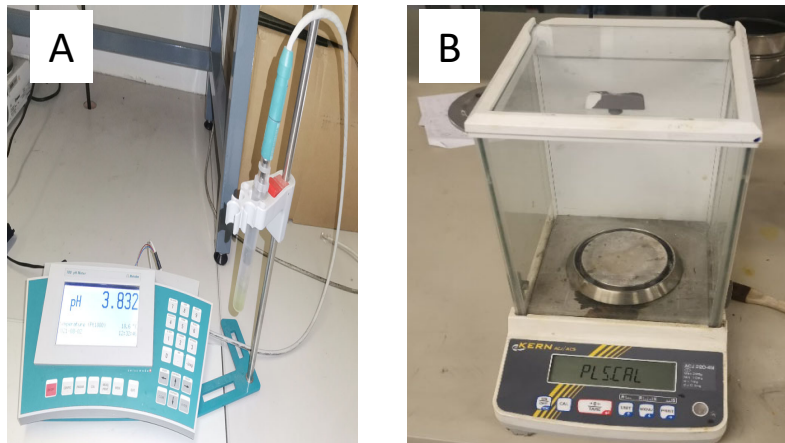


**Figure 3.5:** (A) Metrohm 780 pH meter; (B) Kern ACJ 220-4M analytical balance

### 3.2.6. Hydrogen generation procedure

Hydrogen generation by hydrolysis was studied using our in-house built set-up at the University of the Western Cape. Figure 3.6 shows the complete experimental set-up used for hydrolysis experiments. For each hydrolysis, experiment the reaction solution 40ml were placed inside the 5 neck borosilicate flat-bottom jacket reactor vessel; the temperature of the reaction solution was measured using a k-type thermocouple, which was inserted inside the flask through one of its necks. The hydrolysis experiments were performed at different temperatures by setting the thermostatic bath and passing the water around the reactor vessel. Once the desired temperature was reached for the hydrolysis experiment, the substrate was added (200 mg) to the reaction vessel through the centre neck. A hydrogen output pipeline was attached to another neck of the flask. During the hydrolysis reaction, hydrogen generated in the 5 neck reactor vessel flows through a tube, a moisture absorbent and flowmeters connected to a data logger. The data logger recorded the measurements every 5 seconds using the PC. Different reaction substrates, temperature and composition of hydrolysis

solution were used in this study and are elaborated on and discussed in Chapter 4.

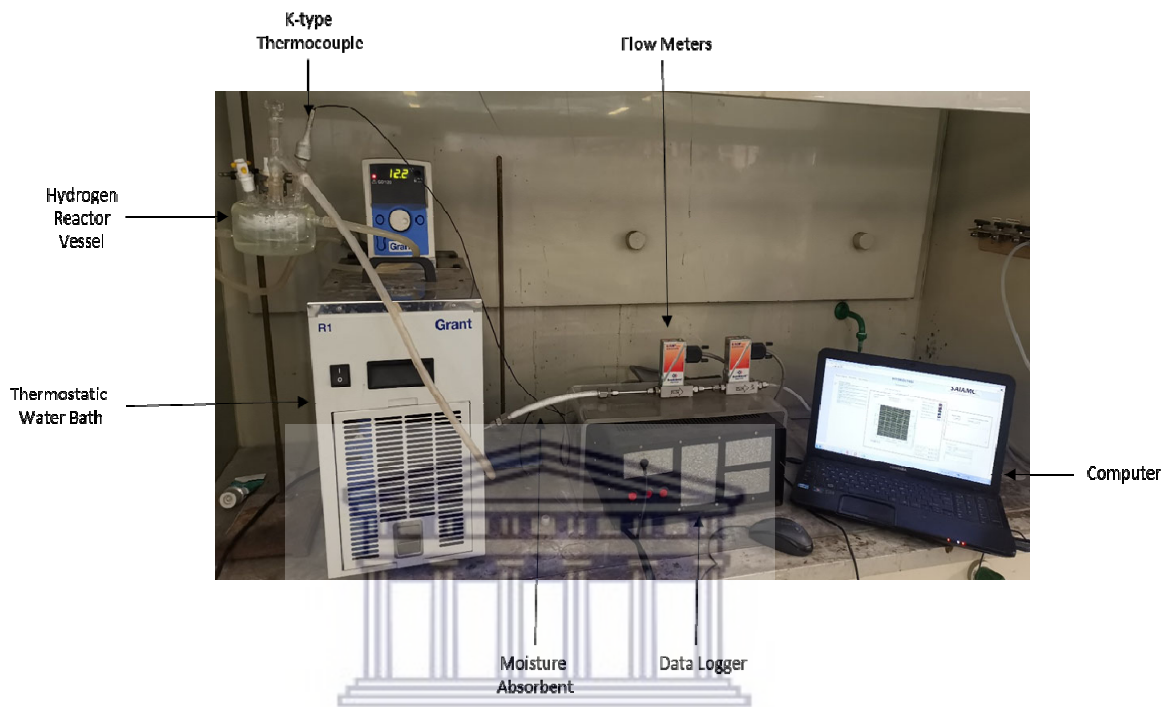


**Figure 3.6:** Experimental set-up for hydrogen generation via hydrolysis

### 3.3. Planetary Ball Milling

Planetary ball mills (such as the one used in this study) are subjectively lower energy mills when compared to shaker mills. The working mechanism of a planetary ball mill consists of one to four milling bowls/vials seated on a rotating disc. During operation, the disc and the milling vials rotate in the opposite direction, resulting in alternately synchronized centrifugal forces [67]. In terms of movement, this translates to the milling balls sliding along the vial walls before falling across and colliding with the opposite side of the vial. Suryanarayana, in his review of mechanical alloying and milling [68], terms these forces as friction forces



(balls sliding along the vial wall) and impact forces (balls flying across the vial and striking the opposite side of the vial), as shown in Figure 3.7.

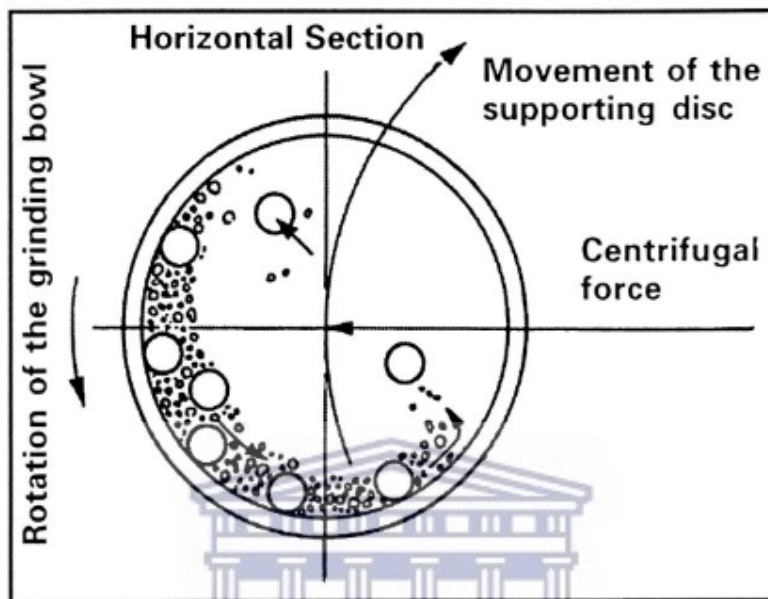


**Figure 3.7:** Schematic showing the movement of the milling vial (grinding bowl) and the rotating disc during milling operations [68].

Synthesis of nanocomposite hydrogen generation substrates in this study was done through ball milling. Ball milling (BM) of magnesium hydride was done using a Fritsch F6 Planetary mill loaded in a stainless steel vial and stainless steel balls shown in Figure 3.8. The ball to powder ratio of 40:1 was employed in all ball-milling experiments. All ball milling experiments were performed under  $H_2$  atmosphere 30 bar at a rotational speed of 500 rpm. The loading and unloading of all milled samples were done inside an argon purified and purged glove box (MBraun-MB200B) to prevent oxidation.

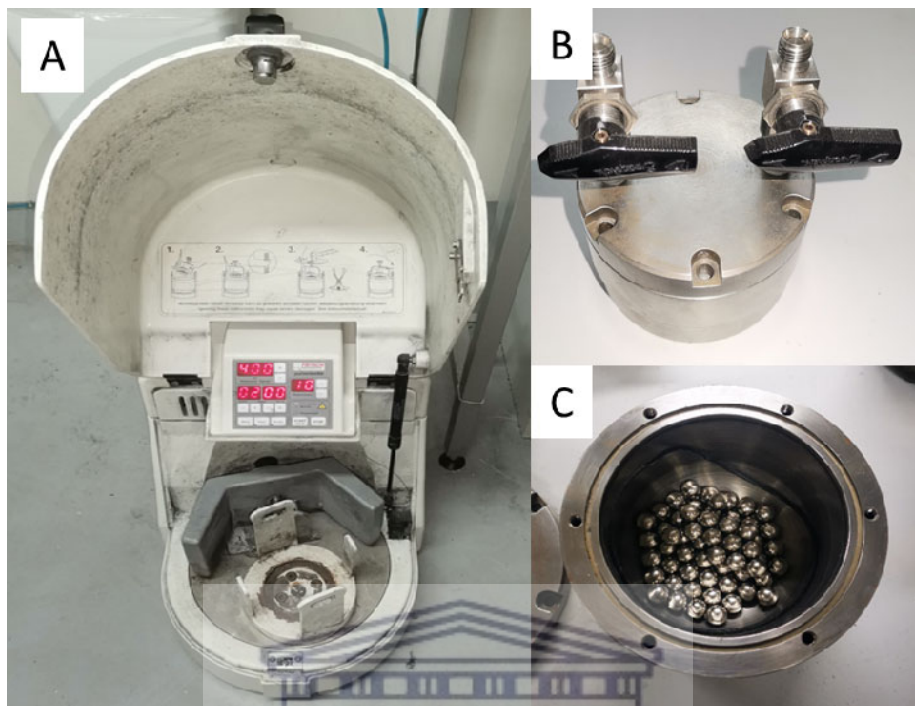


**Figure 3.8:** (A) Fritsch ball mill, (B) Stainless steel vial and (C) Stainless steel balls

### 3.4. Materials Characterization

For this work, several methods of characterization were used to evaluate the as-received and as-prepared  $\text{MgH}_2$  substrates for hydrogen generation via hydrolysis.

#### 3.4.1. Scanning electron microscopy (SEM) & Energy-Dispersive X-Ray Spectroscopy (EDS)

Scanning electron microscopy (SEM) analysis was performed on samples to evaluate the  $\text{MgH}_2$  and its prepared substrates in terms of surface morphology, topography, and composition. In this study, the SEM equipment used was a Zeiss Auriga Field Emission Gun (FEG) SEM with InLens (working distance 5 mm) and

secondary electron, SE (10 mm) detectors operated at an extra high tension (EHT) voltage of 5kV for high-resolution imaging.

SEM typically offers a large depth of focus, allowing for a larger part of the sample to be viewed at a time. The high-resolution imaging enabled the effective examination of formations in close proximity even at high magnifications with little image distortion. The electron beam produced by the equipment interacts with the sample particle and produces secondary or back-scattered electrons that are picked up and recorded by several detectors situated around the sample. The data from these interactions (electron energy, angle of scattering etc.) is then processed and a contrast-based image is produced

For SEM analysis, samples were placed on sticky carbon discs (pre-refrigerated to maintain the crispness of the carbon layer) glued on stubs. The samples were then coated with a gold layer using a gold coating machine to enhance conductivity and adhesion to the carbon surface.

EDS analysis was also performed on the samples for the characterization of their elemental composition. Higher EHT settings (15-20kV) were used for EDS analysis and the secondary electron viewing method was used to locate the suitable area. Once the desired area was selected, the coating type and spectrum were identified so as not to interfere with the compositional analysis of the sample materials.

### **3.4.2 X-Ray Diffraction (XRD)**

This analytical technique is used primarily for phase identification of crystalline material. It is a powerful technique used for solids characterization and

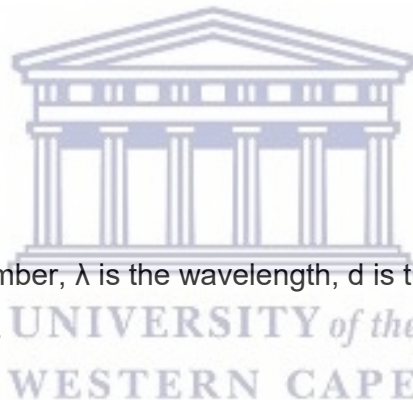


provides information on unit cell dimensions. XRD analysis was used to evaluate the composition and crystalline properties of the as-received substrates and the substrates after hydrolysis experiments.

The working principle is that crystal plane atoms arise as a result of bombarding crystalline solids with a collimated x-ray beam, x-ray is then diffracted in numerous angles. Diffraction at only one angle gives it unique characteristics with crystal planes (hkl) and inter-plane spacing ( $d_{hkl}$ ). The diffraction angle is defined from Bragg's law equation 1, where the intensities of the diffracted x-ray are measured and plotted against corresponding Bragg angles ( $2\theta$ ) to produce a diffractogram.

$$n\lambda = 2d\sin\theta \quad [3.1]$$

Where, n is the order number,  $\lambda$  is the wavelength, d is the basal spacing (Å) and  $\theta$  the diffraction angle (°).



In this work, all XRD analysis were performed at iThemba Labs. All analyses were performed using a Bruker AXS D8 Advanced diffractometer with Cu-K $\alpha$  radiation ( $\lambda_1=1.5406$  Å,  $\lambda_2=1.5444$  Å,  $\lambda_2/\lambda_1=0.5$ ). The instrument was water-cooled and employed a Bragg angle,  $2\theta$  of 10 – 90°. The scan rate and step size used were 1.2°/min and 0.035°, respectively. To determine the instrument contribution towards peak profiles, a standard  $\alpha$ -Al<sub>2</sub>O<sub>3</sub> sample was used as a calibration background profile. After that, the Rietveld full profile analysis of the data was achieved using the General Structure Analysis System (GSAS) software.

### 3.4.3 Thermogravimetric Analysis (TGA) / Differential scanning calorimetry (DSC)

Thermogravimetric analysis (TGA) and differential scanning calorimetry (DSC) was carried out on the as-received and ball-milled  $\text{MgH}_2$  samples using a Perkin Elmer STA 8000 thermal analyzer. For this analysis, a small amount of sample was weighed out (typically between 10 and 30 mg) into the ceramic crucible and the sample chamber was continuously purged with pure argon gas at 100 ml/min to eliminate oxidants and flush away hydrogen that evolves from the sample. The samples were heated from 30 °C to 600 °C at a heating rate of 10 °C/min, before cooling down to 30 °C again.

TGA analysis is typically shown as a profile of sample weight against temperature. Because hydrogen is reversibly absorbed onto the Mg composite, it desorbs from the sample at a specific temperature (hydrogen desorbs from pure  $\text{MgH}_2$  at approximately 300 °C) and can be traced as weight lost from the sample. This provides a good assessment of hydrogen interaction with the sample.

DSC analysis involved tracking the heat flow into the sample against the temperature of the sample itself. The results from the DSC analysis can be used to calculate the activation energy of hydrogen evolution from the sample via the Kissinger method.

### 3.4.4 Sievert Apparatus

There are two methods that can be used to study the sorption kinetics of metal hydrides. The gravimetric method measures the changes in material weight

as a means to quantify the absorption/desorption of hydrogen from the material. Due to the intrinsic nature of hydrogen (incomparably lightweight), a highly sensitive micro-balance is required and can only be performed using complicated and expensive equipment. The second method, and the method used in this study, is the volumetric method (Sievert's method). The Sieverts method uses a set-up that measures pressures and temperatures in a known fixed volume within a closed system. The Sieverts method is widely preferred due to its simpler, cheaper and user-friendly equipment requirements.

In the study, an in-house built Sievert-type apparatus was used to study the hydrogen desorption (dehydrogenation) and absorption (re-hydrogenation) is shown in Figure 3.9 below [3].

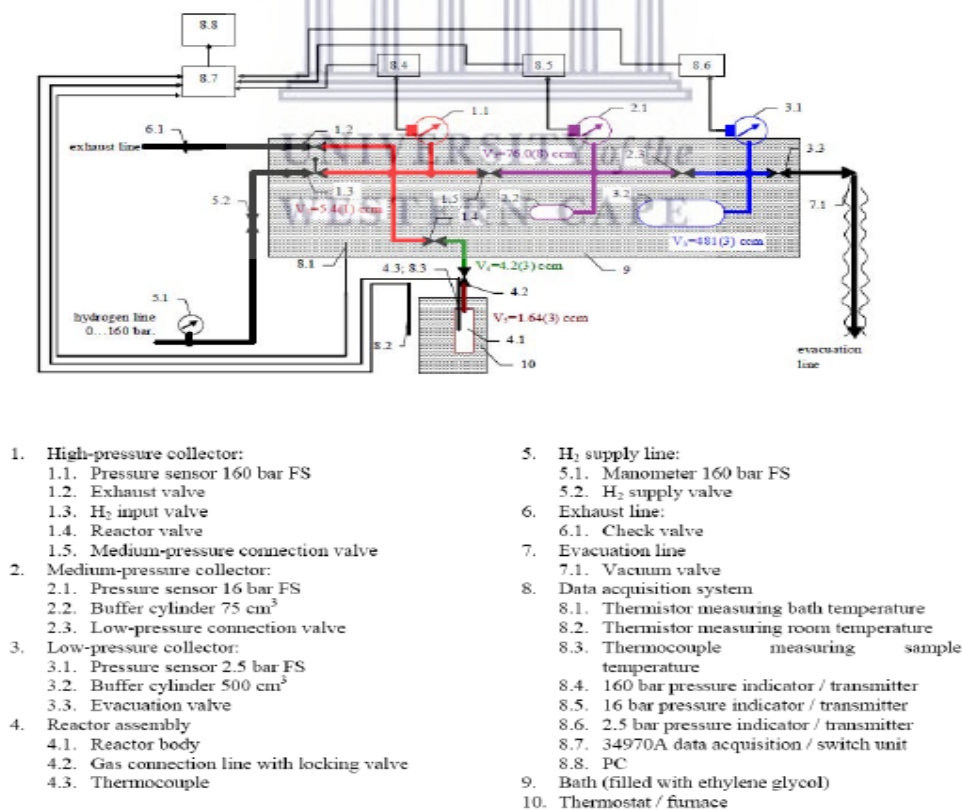


**Figure 3.9:** Schematic diagram of Sievert apparatus installation at SAIAMC

### 3.4.5. Thermal Desorption Studies (TDS) and re-hydrogenation

The hydrogen sorption studies of the as-received  $\text{MgH}_2$  were studied using Sievert's apparatus to assess the materials performance in terms of hydrogen release and uptake. The sample weighing approximately 200 – 400 mg was loaded into the reactor inside of an argon-purged glove box to avoid oxidation and contamination of the sample. The entire reactor and Sieverts apparatus was then evacuated at room temperature to  $<10^{-4}$  mbar vacuum pressure. TDS measurements were carried out by heating the sample from room temperature to 450 – 470 °C under dynamic vacuum at a rate of 5 °C/min. When hydrogen desorption occurs, the vacuum pressure is affected and is thus translated into meaningful desorption data. The TDS procedure was halted once the vacuum pressure returned to its original value, i.e. hydrogen desorption was complete.

For the re-hydrogenation of samples, the reactor (still connected to the Sieverts' apparatus after TDS) was cooled down to 250 °C with an initial hydrogen pressure of 12 – 15 bar. The final pressure after absorption using the abovementioned amount of sample is typically 6 – 8 bar. Hydrogen absorption data during re-hydrogenation was processed using the Avrami-Erofeev equation to interpret kinetics:

$$C = C_{max} \left\{ 1 - \exp \left[ - \left( \frac{t}{t_0} \right)^n \right] \right\} \quad [3.2]$$

Where C is the actual hydrogen absorption,  $C_{max}$  is the maximum hydrogen absorption, t is time,  $t_0$  is the characteristic hydrogenation time or reciprocal rate constant and n is an exponential factor indirectly related to the reaction mechanism

---

## Results and Discussion

---

This chapter discusses the results obtained for the investigation of  $\text{MgH}_2$  and  $\text{NaAlH}_3$  for hydrogen generation via hydrolysis. The hydrolysis experiments were performed in de-ionized water and different organic acid solutions. This section will outline all the results, discussions, and a summary of all the findings obtained in this study.

### 4.1. Characterization of as received $\text{MgH}_2$

In this section of the study, a complete characterization of the as-received  $\text{MgH}_2$  was carried out, such as SEM, XRD, TGA/DSC, hydrogen absorption and  $\text{H}_2$  production via hydrolysis. This investigation was conducted to serve as a benchmark for the analysis to follow.

#### 4.1.1. Scanning electron microscope (SEM) and Energy dispersive X-ray spectroscopy (EDS) of the as-received $\text{MgH}_2$

The SEM images of the as-received  $\text{MgH}_2$  at different magnifications are shown in Figures 4.1 (A) and (B). The morphology of the as-received  $\text{MgH}_2$  shows an irregular and flaky particle orientation. This is similar to an observation by Varin et al. about  $\text{MgH}_2$  as-received from industry [69].

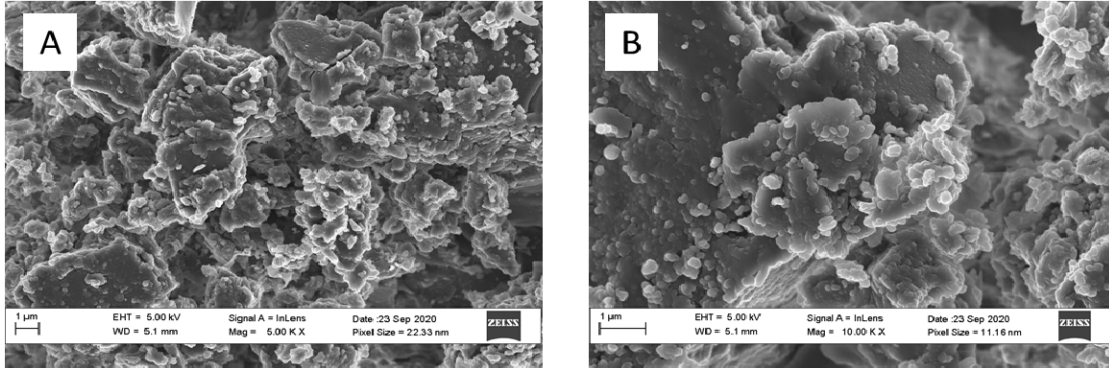


**Figure 4.1:** SEM images of the as-received  $MgH_2$

EDS studies performed in this work, provide elemental compositions for various materials and their compounds, as shown in Figure 4.2 and Table 4.1. From the EDS spectra, it can be observed that there are three elements present in the as-received  $MgH_2$  these are magnesium (Mg), oxygen (O) and carbon (C). The carbon is not actually part of the sample's composition; it shows up in the spectra because carbon adhesive tape is used to allow the sample to adhere to the stub. The Mg represents the major constituent expected in the sample with weight and atomic compositions of 90.88 and 86.98 %, respectively. The oxygen present in the sample is probably due to the oxidation of the  $MgH_2$ .

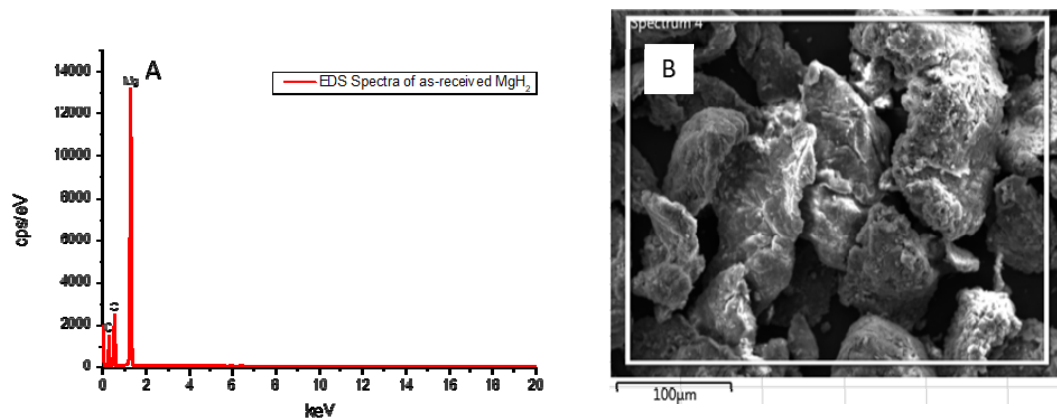


**Figure 4.2:** (A) EDS spectra of as-received  $MgH_2$ , (B) area of the EDS

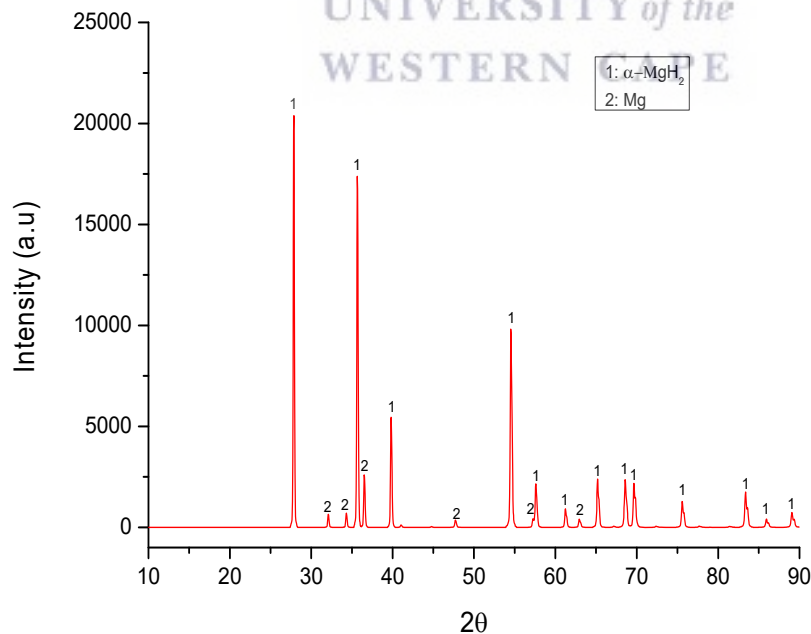


**Table 4.1:** Elemental composition of as – received MgH<sub>2</sub>

Elements	Weight %	Atomic %
Mg	90.88	86.98
O	9.12	13.02
Total	100	100

#### 4.1.2. X-Ray diffraction (XRD) analyses of the as-received MgH<sub>2</sub>

XRD analysis was conducted on the as-received MgH<sub>2</sub> to provide information on the materials structural properties, which was used as hydrogen generation substrate. The XRD pattern for the as-received MgH<sub>2</sub> is shown in Figure 4.3; two major phases were observed, namely  $\alpha$ -MgH<sub>2</sub> and Mg. From the XRD pattern, it can be seen that the as-received MgH<sub>2</sub> used in this study consists of the tetragonal  $\alpha$ -MgH<sub>2</sub> as the predominant phase, also the MgO phase usually associated with MgH<sub>2</sub> due to oxidation is not present in the sample.

**Figure 4.3:** XRD pattern for the as-received MgH<sub>2</sub>

### 4.1.3. Thermogravimetric analysis (TGA) and Differential scanning calorimetry (DSC) analysis of as-received $\text{MgH}_2$

The TGA and DSC results of the as-received  $\text{MgH}_2$  are presented in Figure 4.4. The TGA results show that the decomposition of the as-received  $\text{MgH}_2$  started at around 400 °C with a total dehydrogenation capacity of 6.8 wt.% at 450 °C. After dehydrogenation, there is a slight increase in weight, which is due to oxidation. The DSC results for the as-received  $\text{MgH}_2$  is characterized by a narrow and sharp peak of dehydrogenation. The onset temperature for dehydrogenation is at 400 °C, with a maximum peak at 415 °C and the end peak at 455 °C.

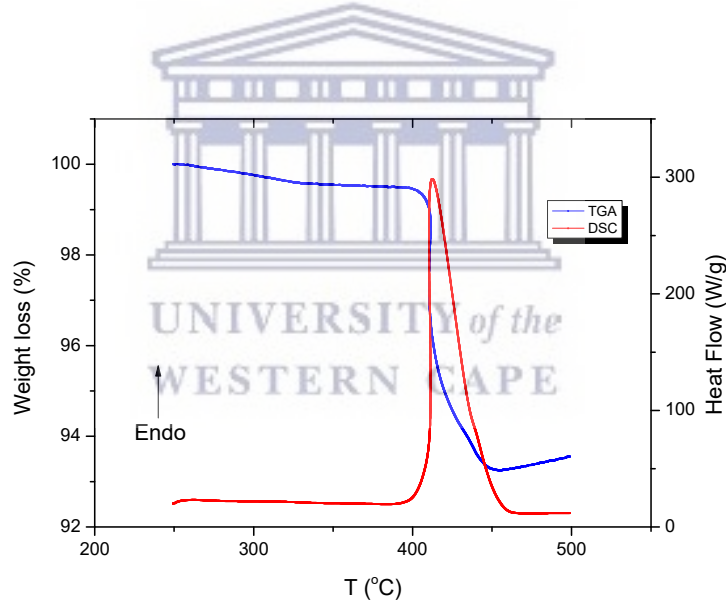


**Figure 4.4:** TGA and DSC analysis of as-received  $\text{MgH}_2$



#### 4.1.4. TDS and Re-hydrogenation of Commercial MgH<sub>2</sub>

Figure 4.5 (A) shows the thermal desorption spectra for as-received MgH<sub>2</sub>, which was heated at a heating rate of 5 °C/min under vacuum. The first TDS decomposition of the as-received MgH<sub>2</sub> shows an onset decomposition temperature,  $T_{onset}$ , at 460 °C with a sharp endothermic peak ( $T_{max}$ = 488 °C) followed by a sharp decrease of the decomposition rate. The peak temperature for the second TDS for the as-received MgH<sub>2</sub> was lowered by ~ 73 °C to that of the first TDS for the as-received MgH<sub>2</sub>, having an onset temperature and peak temperature at 350 °C and 415 °C, respectively.

The re-hydrogenation results for the as-received MgH<sub>2</sub> after TDS and their kinetics curves (H<sub>2</sub> wt. % vs time) at 300 °C (~15 bar H<sub>2</sub>) are shown in Figure 4.5 (B). The results show that the as-received MgH<sub>2</sub> has very sluggish H<sub>2</sub> absorption kinetics due to its low H<sub>2</sub> capacity uptake of only 3.2 wt. % for the first re-hydrogenation. The second re-hydrogenation, the material only absorbed 2.8 wt. % H<sub>2</sub> this low H<sub>2</sub> uptake can be attributed to the high (above 500 °C) dehydrogenation temperature, which can result in a deterioration of re-hydrogenation kinetics due to sintering and recrystallization of Mg, in-turn slowing down H<sub>2</sub> diffusion through the Mg layer.

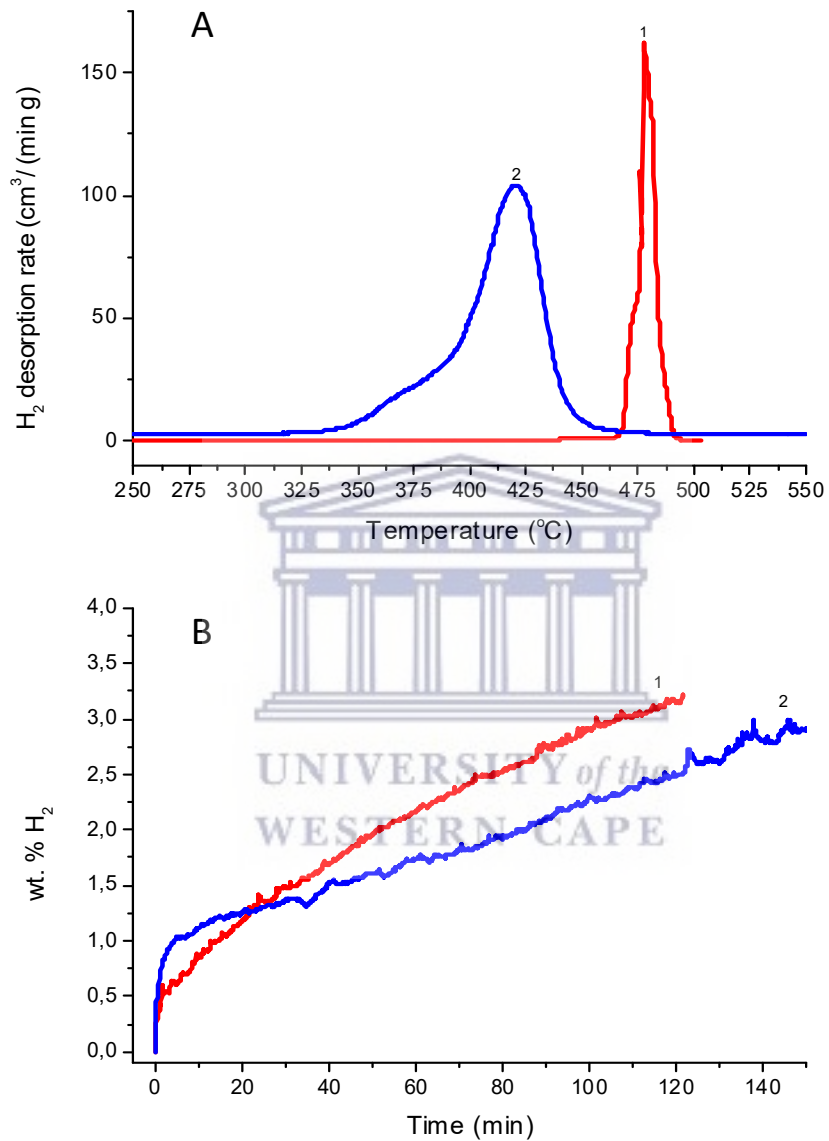


**Figure 4.5:** (A) TDS of commercial MgH<sub>2</sub> (1) 1st TDS and (2) 2nd TDS, (B) re-hydrogenation of commercial MgH<sub>2</sub> (1) 1st re-hydrogenation and (2) 2nd re-hydrogenation.

#### 4.1.5. Hydrolysis of the as-received $\text{MgH}_2$ at different temperature

The Hydrolysis of the as-received  $\text{MgH}_2$  was performed at 25, 50, and 75 °C in de-ionized water. The results of the  $\text{H}_2$  generation from the experiments are presented in Figure 4.6. The hydrogen production is expressed as hydrogen yield (%), defined as the volume of produced  $\text{H}_2$  over the theoretical volume of hydrogen that should be released assuming that all material is hydrolyzed. As expected, the elevation of the hydrolysis temperature leads to an increase both in the reaction rates and in the hydrogen yields. From Figure 4.5, it can be seen that for the as-received  $\text{MgH}_2$  during hydrolysis at 25, 50 and 75 °C, the hydrogen yield was 3.35, 12.75 and 23.77 %, respectively. The reason for the increase in the yield of hydrogen produced at elevated temperatures can be attributed to the reduction of passivation caused by the production of  $\text{Mg}(\text{OH})_2$  due to high reaction temperature.

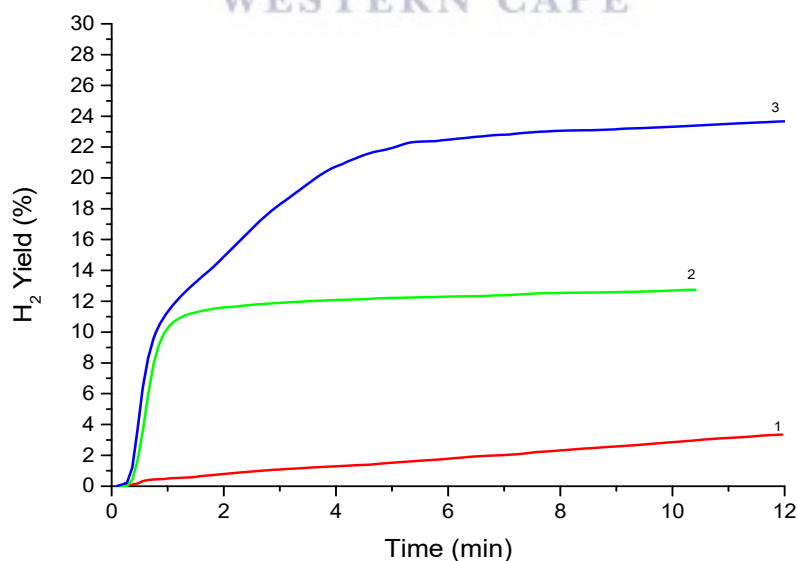


**Figure 4.6:** Effect of temperature on the Hydrolysis of  $\text{MgH}_2$ , (1) 25 °C, (2) 50 °C, (3) 75 °C.

#### 4.1.6. X-ray diffraction (XRD) analyses of ball milled MgH<sub>2</sub>

Figure 4.7 shows the XRD plots of as-received MgH<sub>2</sub> ball milled for 2, 4 and 6 hours stacked for easy comparison. From the plots, it can be observed that after ball milling of MgH<sub>2</sub> in H<sub>2</sub>, it results in complete hydrogenation of the residual Mg, which leads to the formation of  $\gamma$ -MgH<sub>2</sub> in addition to  $\alpha$ -MgH<sub>2</sub>. This was also reported in the literature [70]. Moreover, from Table 4.2, it can be seen that the as-received MgH<sub>2</sub> has two phases,  $\alpha$ -MgH<sub>2</sub> and Mg, while the ball milled MgH<sub>2</sub> samples has three phases, namely  $\alpha$ -MgH<sub>2</sub>,  $\gamma$ -MgH<sub>2</sub> and MgO. The increase in nanocrystalline MgO is mainly caused during long-time ball milling due to oxidation of Mg/MgH<sub>2</sub> due to ambient air intrusion into the vial during milling or oxidation of the sample when preparing the sample and taking its XRD. From a structural perspective, the XRD plots in Figure 4.7 show the broadening of the peaks in the ball milled samples and shifting of peaks to the right compared to the as-received MgH<sub>2</sub>, which indicates the reduction of crystallinity of the material.

From the Rietveld analysis using GSAS software, the crystallite phase ( $\alpha$ -MgH<sub>2</sub>) in the as-received MgH<sub>2</sub> reduced from over 1000 nm to about 9 nm after ball milling in H<sub>2</sub>. This reduction in crystallite size of the  $\alpha$ -MgH<sub>2</sub>, as well as the formation of Mg to  $\gamma$ -MgH<sub>2</sub>, is responsible for the higher H<sub>2</sub> evolution from the ball mill MgH<sub>2</sub> Hydrolysis when compared to the as-received MgH<sub>2</sub>.

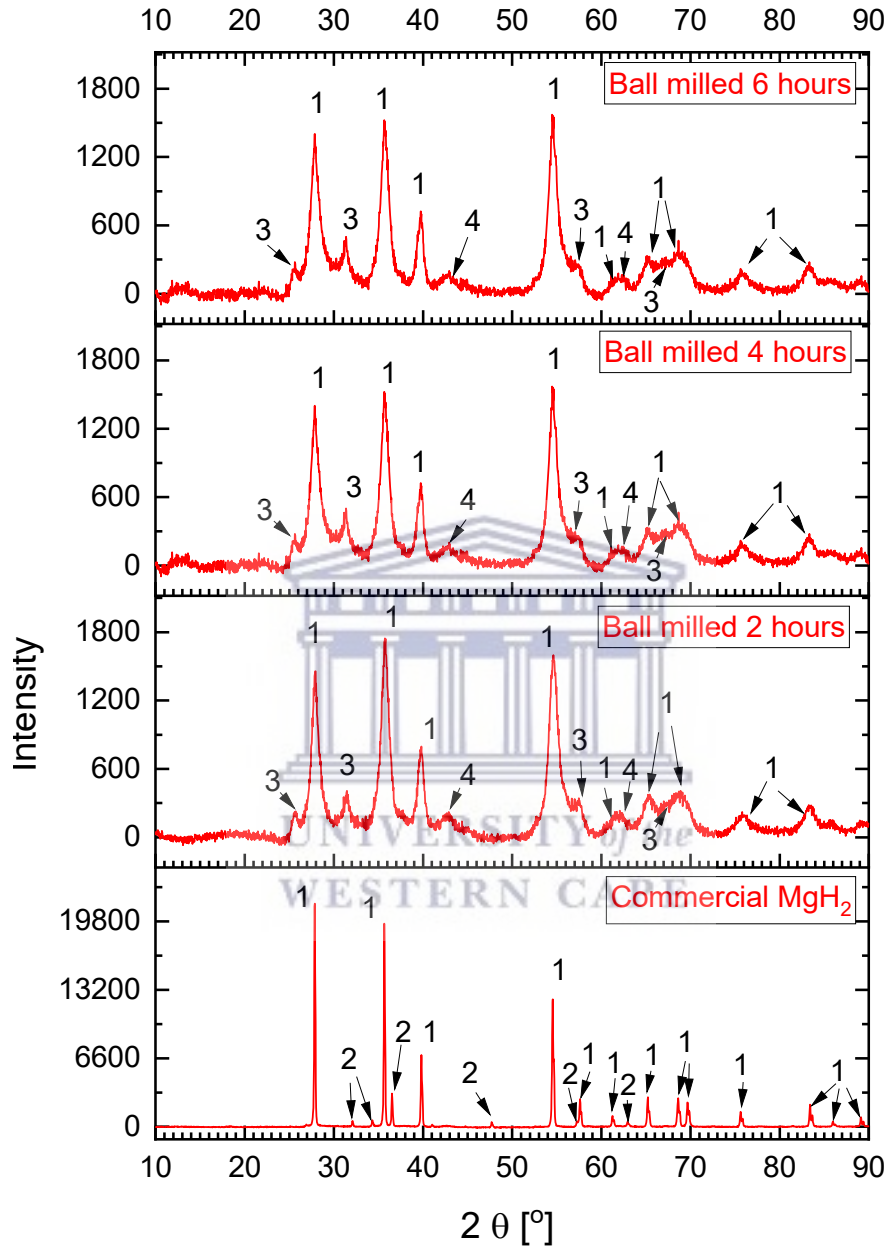


**Figure 4.7:** XRD patterns of as-received  $MgH_2$  and  $MgH_2$  ball milled in  $H_2$  for different times. Peak labels: 1 –  $\alpha$ - $MgH_2$ , 2 – Mg, 3 –  $\gamma$ - $MgH_2$ , 4 – MgO. Intensities (Y-axis) are shown in arbitrary units (same for all the patterns).

**Table 4.2:** Results of Rietveld refinement of the studied samples

Sample	Phase	Weight abundance	Lattice periods [Å]			Unit cell volume [Å <sup>3</sup> ]	Estimated crystallite size [nm]
			<i>a</i>	<i>b</i>	<i>c</i>		
Com. MgH <sub>2</sub> (as delivered)	α-MgH <sub>2</sub>	0.909(-)	4.51838(6)	4.51838(6)	3.02222(7)	61.701(2)	>1000
	Mg	0.091(2)	3.2134(2)	3.2134(2)	5.2146(7)	46.633(8)	~1000
MgH <sub>2</sub> ball milled in H <sub>2</sub> for 2 hours	α-MgH <sub>2</sub>	0.752(-)	4.5240(5)	4.5240(5)	3.0283(6)	61.98(2)	9
	γ-MgH <sub>2</sub>	0.175(3)	4.538(3)	5.460(4)	4.958(3)	122.8(2)	13
	MgO	0.073(3)	4.225(3)	4.225(3)	4.225(3)	75.4(1)	8
MgH <sub>2</sub> ball milled in H <sub>2</sub> for 4 hours	α-MgH <sub>2</sub>	0.740(-)	4.5255(6)	4.5255(6)	3.0292(7)	62.04(2)	9
	γ-MgH <sub>2</sub>	0.225(4)	4.544(4)	5.488(6)	4.962(5)	123.8(2)	10
	MgO	0.035(3)	4.223(4)	4.223(4)	4.223(4)	75.3(2)	12
MgH <sub>2</sub> ball milled in H <sub>2</sub> for 6 hours	α-MgH <sub>2</sub>	0.653(-)	4.5265(5)	4.5265(5)	3.0313(6)	62.11(2)	9
	γ-MgH <sub>2</sub>	0.141(4)	4.555(7)	5.466(9)	4.973(8)	123.8(3)	8
	MgO	0.206(3)	4.248(2)	4.248(2)	4.248(2)	76.63(9)	6

**Table 4.3:** Reference data for the phases identified during Rietveld refinement of the XRD patterns

Phase	Space group	Lattice periods [Å]			Reference
		<i>a</i>	<i>b</i>	<i>c</i>	
α-MgH <sub>2</sub>	<i>P4</i> <sub>2</sub> / <i>mnm</i> (136)	4.5147	4.5147	3.0193	[71]
Mg	<i>P6</i> <sub>3</sub> / <i>mmc</i> (194)	3.211	3.211	5.213	[72]
γ-MgH <sub>2</sub>	<i>Pbcn</i> (60)	4.5139	5.4391	4.9406	[71]
MgO	<i>Fm</i> - <i>3m</i> (225)	4.212	4.212	4.212	[73]

#### 4.1.7. Hydrolysis of ball milled MgH<sub>2</sub>

Mechanical ball milling of substrates for hydrogen generation and storage is a well-known method to reduce some of the kinetic and thermodynamic limitations experienced in hydrogen generation and solid-state hydrogen storage materials. Ball milling normally increases the specific surface area of the material and increases the crystallite size of the material, and enhances nucleation in the metals crystals due to fracturing of the crystals [74]. In this section of the study, H<sub>2</sub> production from the as-received MgH<sub>2</sub> was compared with the same material ball milled for 2, 4 and 6 hrs. The effect of ball milling on the Hydrolysis of MgH<sub>2</sub> reactivity in de-ionized water is shown in Figure 4.8. From Figure 4.8, it is observed that as the milling time increase, the hydrogen yield also increases. The H<sub>2</sub> yield for 2, 4 and 6 hrs milling time are 17.58, 19.74 and 21.09 %, respectively compared to 3.35 % for unmilled MgH<sub>2</sub>. M.H Grosjean et al. showed that as one increases the milling time of MgH<sub>2</sub> for hydrolysis, the conversion yield of H<sub>2</sub> also increases due to the increase in the specific area of the powder by ball milling [75].

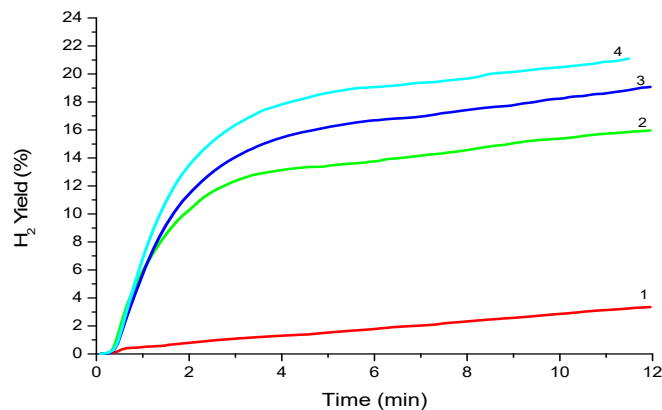
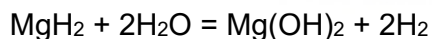


**Figure 4.8:** Hydrogen generation of ball milled MgH<sub>2</sub> (1) as-received MgH<sub>2</sub>, (2) 2 hrs ball milled MgH<sub>2</sub>, (3) 4 hrs ball milled MgH<sub>2</sub>, (4) 6 hrs ball milled MgH<sub>2</sub>

## 4.2. Effect of Organic Acid on the Hydrolysis of MgH<sub>2</sub>

In this section, the effect of different organic acids was studied to understand how they influence the Hydrolysis of MgH<sub>2</sub>. MgH<sub>2</sub> is a light grey crystalline powder that releases H<sub>2</sub> at a high temperature above 320 °C under normal pressure. On contact with water, it decomposes slowly to form H<sub>2</sub> gas and magnesium hydroxide. The Mg(OH)<sub>2</sub> layer acts as a passive layer that hinders the generation of H<sub>2</sub> gas. To accelerate the rate of H<sub>2</sub> generation, acids can be used to serve as a pH buffer. Previously, hydrochloric acid was used to catalyze the hydrolysis reaction of MgH<sub>2</sub>; however, strong acids are not advisable, as it is not environmentally sound and can produce vigorous, sometimes uncontrollable reactions. In this, study three non-toxic acids, such as Acetic, Citric and Oxalic acid, were studied to see the effect they would have on the Hydrolysis of MgH<sub>2</sub>.

The possible chemical transformation equation for the MgH<sub>2</sub> hydrolysis reaction process can be written as:



Where the passivation layer, Mg(OH)<sub>2</sub>, is a weak alkali with a low solubility in water. From literature, pH can be calculated manually using the following equation:

$$\text{pH} = 14 - 1/2\text{pK}_1 + 1/2\log(\text{C})$$

where pK<sub>1</sub> is the basicity constant of Mg(OH)<sub>2</sub> and is given as 2.58 and C is the Mg(OH)<sub>2</sub> concentration.



#### 4.2.1. Effect of Acetic acid on hydrogen evolution by Hydrolysis of MgH<sub>2</sub>

The chemical reaction between MgH<sub>2</sub> and water can be described as a reaction in equation 4.1. From equation 4.1, it can be seen that a Mg(OH)<sub>2</sub> passivation layer is formed during hydrolysis. To accelerate the hydrolysis of MgH<sub>2</sub> for H<sub>2</sub> generation and avoid the passivation layer's generation, acetic acid was used. The reaction of acetic acid with Mg(OH)<sub>2</sub> is shown in equation 4.2, which produces water and magnesium acetate soluble in water.

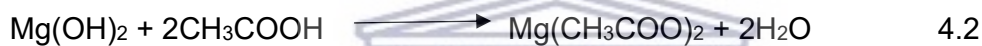
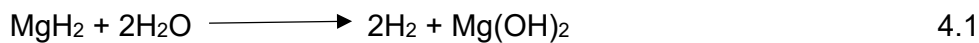
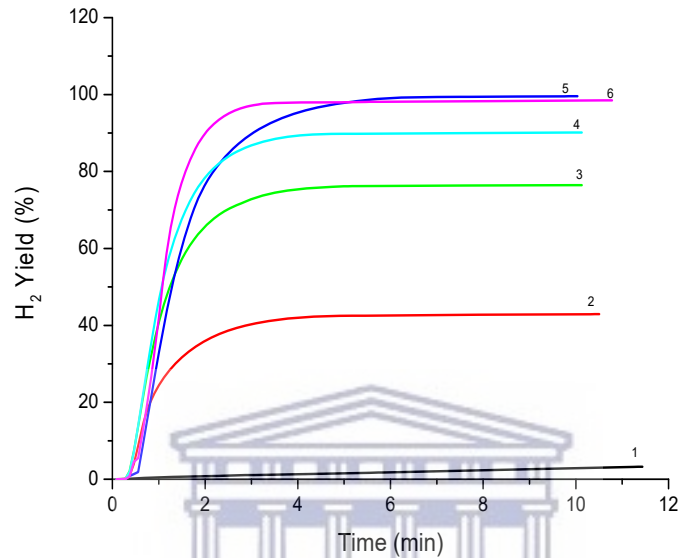


Figure 4.9 shows the H<sub>2</sub> generation from the hydrolysis of MgH<sub>2</sub> with different concentrations of acetic acid 1, 2, 3, 4 and 5 wt.%, respectively. It can be observed that the addition of acetic acid increases the rate of H<sub>2</sub> generation when compared to just de-ionized water. The yield of H<sub>2</sub> produced for 1, 2, 3, 4 and 5 wt.% acetic acid solution is 42.92, 76.47, 90.15, 99.56 and 98.51 %, respectively. From Figure 4.9, it can also be seen that when we increase the concentration of the acetic acid solution, the rate of the reaction and the yield of H<sub>2</sub> generation increase. The hydrolysis of MgH<sub>2</sub> leads to an increase in the pH of the reaction solution; this is due to the release of OH<sup>-</sup> as a result causing the formation of the Mg(OH)<sub>2</sub> passive layer on the surface MgH<sub>2</sub>. From Table 4.4, it can be observed that the Hydrolysis of MgH<sub>2</sub> in de-ionized water the pH increased drastically from 6.55 to 11.04, which is expected due to the Mg(OH)<sub>2</sub> passive layer being formed. However, the addition of acetic acid suppresses the formation of Mg(OH)<sub>2</sub>; this

was mainly due to the initial pH being acidic, which causes less  $\text{OH}^-$  to be released into the solution.



**Figure 4.9:** The effect of acetic acid concentration on  $\text{H}_2$  generation of  $\text{MgH}_2$ , (1) hydrolysis of  $\text{MgH}_2$  in de-ionized water, (2) hydrolysis of  $\text{MgH}_2$  in 1wt. % acetic acid solution, (3) hydrolysis of  $\text{MgH}_2$  in 2 wt. % acetic acid solution, (4) hydrolysis of  $\text{MgH}_2$  in 3 wt. % acetic acid solution, (5) hydrolysis of  $\text{MgH}_2$  in 4 wt. % acetic acid solution, (6) hydrolysis of  $\text{MgH}_2$  in 5 wt. % acetic acid solution.

**Table 4.4:** pH of acetic acid solutions at different concentrations before and after Hydrolysis of  $\text{MgH}_2$  at  $25^\circ\text{C}$ .

	De-ionized water	Acetic Acid				
Concentration		1 wt. %	2 wt.%	3 wt.%	4 wt. %	5 wt.%
Initial pH	6.55	2.95	2.81	2.69	2.64	2.55
Final pH	11.04	5.54	5.28	4.28	4.65	4.51

#### 4.2.2. Effect of Citric acid on hydrogen evolution by Hydrolysis of MgH<sub>2</sub>

The basic hydrolysis reaction between MgH<sub>2</sub>, water and citric acid is shown in eq. 4.3 and 4.4. From the equations, it can be seen that during hydrolysis, the end product Mg(OH)<sub>2</sub> goes into an Arrhenius acid-base reaction which then reacts with the citric acid to produce water and magnesium citrate in aqueous solution.

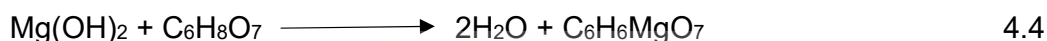
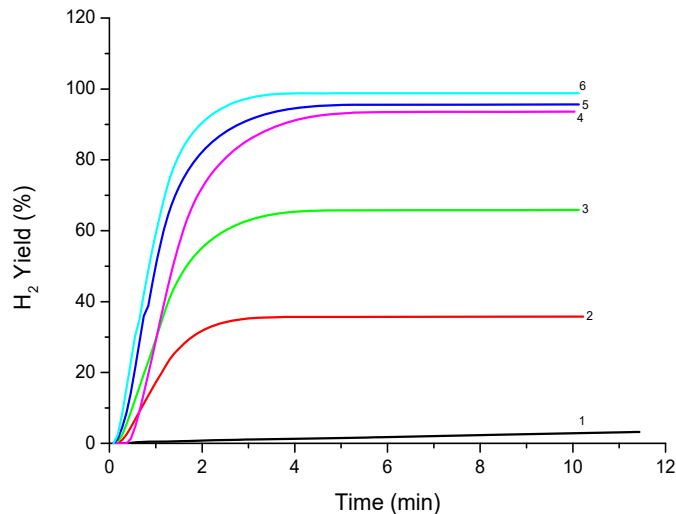


Figure 4.10 shows the H<sub>2</sub> generation from the hydrolysis of MgH<sub>2</sub> with different concentrations of citric acid 1, 2, 3, 4 and 5 wt.%, respectively. It can be observed that the addition of citric acid increases the rate of H<sub>2</sub> generation when compared to just de-ionized water. The yield of H<sub>2</sub> produced for 1, 2, 3, 4 and 5 wt.% citric acid solution is 35.76, 65.87, 93.59, 95.64 and 98.81 %, respectively. From Figure 4.10, it can also be seen that when we increase the concentration of the citric acid solution, the rate of the reaction and the yield of H<sub>2</sub> generation increase. Table 4.5 shows the pH of the reaction solutions with citric acid before and after Hydrolysis of MgH<sub>2</sub>. However, the addition of citric acid suppresses the formation of Mg(OH)<sub>2</sub>; this was mainly due to the initial pH being acidic, which causes less OH<sup>-</sup> to be released into the solution, which leads to faster H<sub>2</sub> generation rate and increased H<sub>2</sub> % yield.



**Figure 4.10:** The effect of citric acid concentration on  $H_2$  generation of  $MgH_2$ , (1) hydrolysis of  $MgH_2$  in de-ionized water, (2) hydrolysis of  $MgH_2$  in 1wt. % citric acid solution, (3) hydrolysis of  $MgH_2$  in 2 wt. % citric acid solution, (4) hydrolysis of  $MgH_2$  in 3 wt. % citric acid solution, (5) hydrolysis of  $MgH_2$  in 4 wt. % citric acid solution, (6) hydrolysis of  $MgH_2$  in 5 wt. % citric acid solution.

**Table 4.5:** pH of citric acid solutions at different concentrations before and after Hydrolysis of  $MgH_2$  at  $25^\circ C$ .

	De-ionized water	Citric Acid				
Concentration		1 wt. %	2 wt.%	3 wt.%	4 wt. %	5 wt.%
Initial pH	6.55	2.43	2.25	2.16	2.09	2.02
Final pH	11.04	5.32	4.98	4.53	4.13	3.86

### 4.2.3. Effect of Oxalic acid on hydrogen evolution by Hydrolysis of MgH<sub>2</sub>

The basic hydrolysis reaction between MgH<sub>2</sub>, water and oxalic acid is shown in eq. 4.4 and 4.5. From the equations, it can be seen that during hydrolysis, the end product Mg(OH)<sub>2</sub> goes into an Arrhenius acid-base reaction which then reacts with the oxalic acid to produce water and dissolved magnesium oxalate.

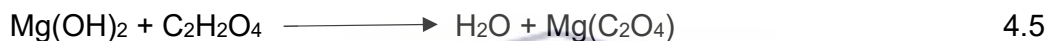
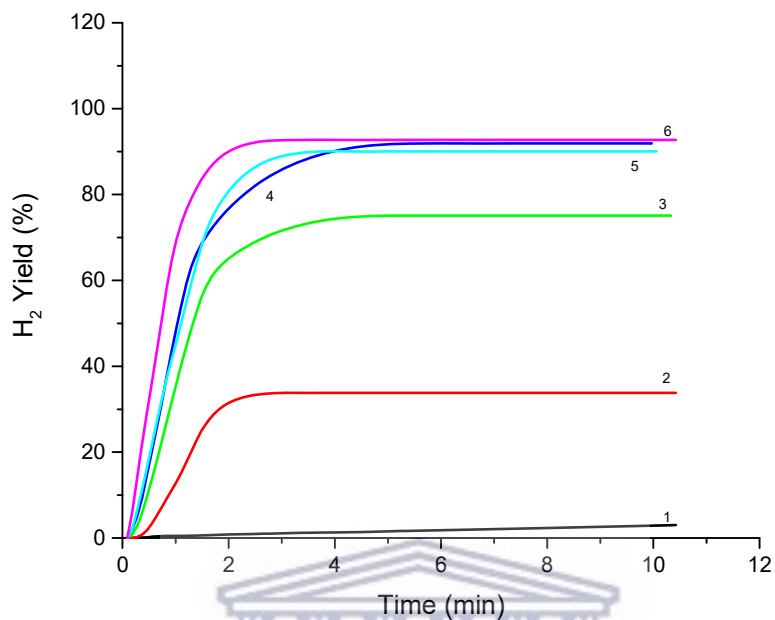


Figure 4.11 shows the H<sub>2</sub> generation from the hydrolysis of MgH<sub>2</sub> with different concentrations of oxalic acid 1, 2, 3, 4 and 5 wt.%, respectively. It can be observed that the addition of oxalic acid increases the rate of H<sub>2</sub> generation when compared to just de-ionized water. The yield of H<sub>2</sub> produced for 1, 2, 3, 4, and 5 wt.% oxalic acid solution is 35.79, 75.09, 91.89, 90.06 and 92.69 %, respectively. From Figure 4.11, it can also be seen that when we increase the concentration of the oxalic acid solution, the rate of the reaction and the yield of H<sub>2</sub> generation increase. Table 4.6 shows the pH of the reaction solutions with oxalic acid before and after Hydrolysis of MgH<sub>2</sub>. The addition of oxalic acid suppresses the formation of Mg(OH)<sub>2</sub>, this was mainly due to the initial pH being acidic, which causes less OH<sup>-</sup> to be released into the solution, which leads to a faster H<sub>2</sub> generation rate and increased H<sub>2</sub> % yield.



**Figure 4.11:** The effect of oxalic acid concentration on  $H_2$  generation of  $MgH_2$ , (1) hydrolysis of  $MgH_2$  in de-ionized water, (2) hydrolysis of  $MgH_2$  in 1wt. % oxalic acid solution, (3) hydrolysis of  $MgH_2$  in 2 wt. % oxalic acid solution, (4) hydrolysis of  $MgH_2$  in 3 wt. % oxalic acid solution, (5) hydrolysis of  $MgH_2$  in 4 wt. % oxalic acid solution, (6) hydrolysis of  $MgH_2$  in 5 wt. % oxalic acid solution.

**Table 4.6:** pH of oxalic acid solutions at different concentrations before and after Hydrolysis of  $MgH_2$  at 25°C.

	De-ionized water	Oxalic Acid				
Concentration		1 wt. %	2 wt.%	3 wt.%	4 wt. %	5 wt.%
Initial pH	6.55	1.53	1.32	1.21	1.13	1.08
Final pH	11.04	4.84	3.32	2.11	1.70	1.54

### 4.3. X-ray diffraction (XRD) analysis of MgH<sub>2</sub> after Hydrolysis in de-ionized water, acetic acid, citric acid and oxalic acid

XRD analysis of the deposits after hydrolysis was performed on MgH<sub>2</sub> after hydrolysis in de-ionized water and different organic acid solutions. There were no solid deposits left for organic acids when the concentration of the organic acid solutions was more than 1 wt. %. Therefore XRD analysis of MgH<sub>2</sub> after hydrolysis in acetic, citric and oxalic acid was from left over solid by-products from 1 wt. % organic acid solutions. Figure 4.12 shows XRD patterns of the deposits after hydrolysis of MgH<sub>2</sub> in de-ionized water and 1 wt.% acetic acid, 1 wt.% citric acid and 1 wt.% oxalic acid solutions. As shown in Figure 4.12, the deposit after hydrolysis in de-ionized water was composed of unreacted  $\alpha$ -MgH<sub>2</sub>, Mg and Mg(OH)<sub>2</sub>. However, the deposits after hydrolysis of MgH<sub>2</sub> in aqueous organic acid solutions only contain very well crystallized (narrower lines as compared to the starting/commercial MgH<sub>2</sub>) unreacted MgH<sub>2</sub>+Mg and no Mg(OH)<sub>2</sub>. This is expected as Mg(OH)<sub>2</sub> will react with acetic, citric and oxalic acid to form the soluble magnesium acetate, magnesium citrate and magnesium oxalate, respectively. Table 4.7 shows the results for Rietveld refinement for the by-product of MgH<sub>2</sub> after hydrolysis in de-ionized water and 1 wt. % organic acid solutions.

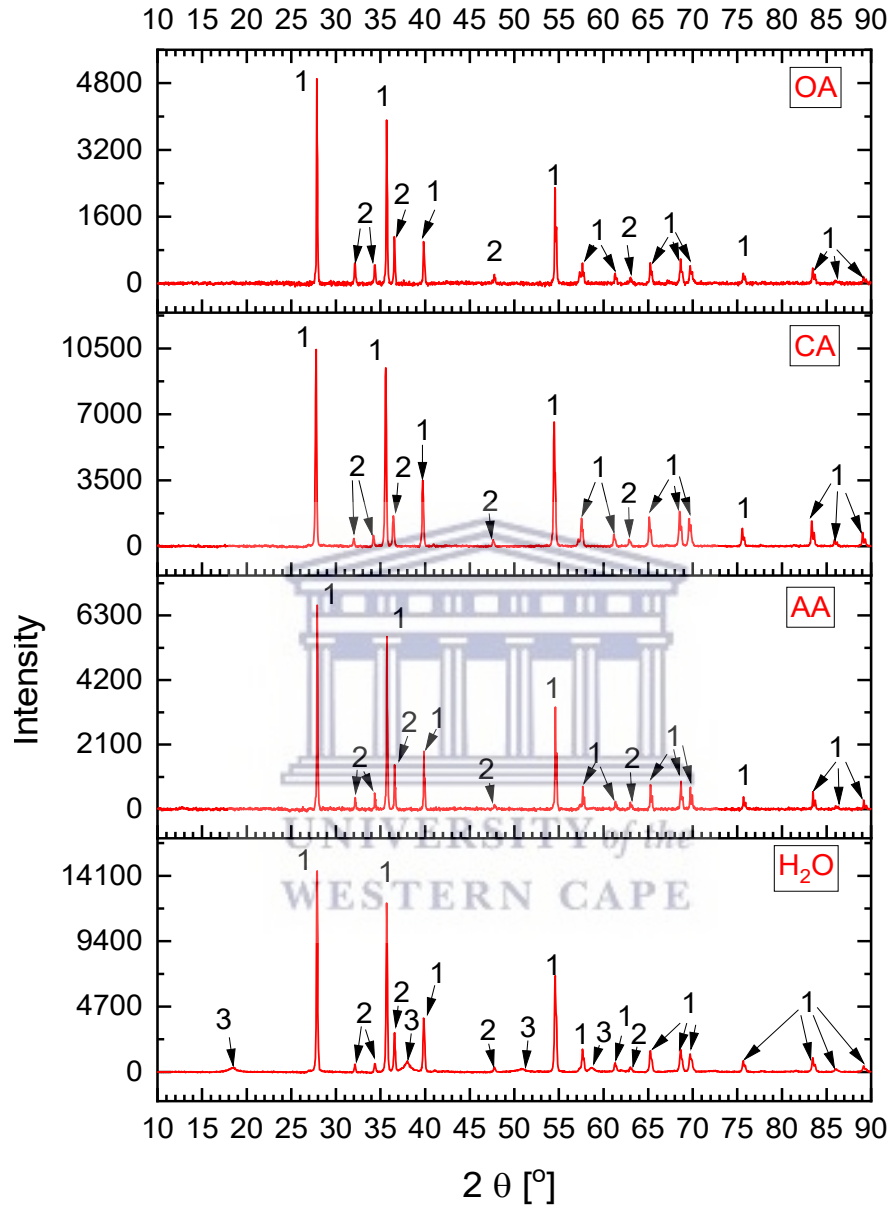


**Figure 4.12:** XRD patterns of the deposit after Hydrolysis of  $MgH_2$  in de-ionized water ( $H_2O$ ) and 1 wt.% aqueous solutions of acetic (AA), citric (CA) and oxalic (OA) acid. Peak labels: 1 –  $\alpha$ - $MgH_2$ , 2 – Mg, 3 –  $Mg(OH)_2$ . Intensities (Y-axis) are shown in arbitrary units (same for all the patterns).



**Table 4.7:** Results of Rietveld refinement of the studied samples

Sample	Phase	Weight abundance	Lattice periods [Å]			Unit cell volume [Å <sup>3</sup> ]	Estimated crystallite size [nm]
			<i>a</i>	<i>b</i>	<i>c</i>		
Deposit after hydrolysis of MgH <sub>2</sub> in deionised water	α-MgH <sub>2</sub>	0.693(-)	4.5156(5)	4.5156(5)	3.0208(6)	61.60(2)	>1000
	Mg	0.090(1)	3.2105(2)	3.2105(2)	5.2101(4)	46.506(5)	>1000
	Mg(OH) <sub>2</sub>	0.217(3)	3.142(1)	3.142(1)	4.787(2)	40.92(2)	11
Deposit after hydrolysis of MgH <sub>2</sub> in acetic acid solution	α-MgH <sub>2</sub>	0.846(-)	4.5152(7)	4.5152(7)	3.0201(8)	61.574(2)	>1000
	Mg	0.154(3)	3.2104(3)	3.2104(3)	5.2116(9)	46.52(1)	>1000
Deposit after hydrolysis of MgH <sub>2</sub> in citric acid solution	α-MgH <sub>2</sub>	0.892(-)	4.5139(6)	4.51393(6)	3.01982(7)	61.530(2)	>1000
	Mg	0.108(2)	3.2101(2)	3.2101(2)	5.2114(7)	46.508(6)	800
Deposit after hydrolysis of MgH <sub>2</sub> in oxalic acid solution	α-MgH <sub>2</sub>	0.818(-)	4.5149(8)	4.5149(8)	3.0197(1)	61.55(2)	>1000
	Mg	0.182(3)	3.2099(2)	3.2099(2)	5.2101(7)	46.49(6)	>1000

#### 4.4. Effect of temperature on the Hydrolysis of MgH<sub>2</sub> in acetic, citric and oxalic acid

In addition to the effect of organic acids on the hydrogen production from the hydrolysis of MgH<sub>2</sub> the temperature also significantly affects the hydrolysis performance. In order to study the effect of temperature on the H<sub>2</sub> generation properties of MgH<sub>2</sub> in organic acid solution, the reaction was carried out in acetic, citric and oxalic acid with the concentration of the solution all kept at 1wt. % and then performing the hydrolysis experiments at different temperatures 25, 50 and 75 °C. Figure 4.13 show the hydrogen generation for the hydrolysis of MgH<sub>2</sub> with (A) 1 wt. % acetic solution, (B) 1 wt. % citric acid solution and (C) 1 wt. % oxalic acid solution at different temperatures. Figure 4.13 (A) shows that 42.90, 74.0 and 97.82 % hydrogen was generated at 25, 50 and 75 °C, respectively. Figure 4.13 (B) shows that 35.76, 55.19 and 70.01 % hydrogen was generated at 25, 50 and 75 °C, respectively. Figure 4.13 (C) shows that 33.79, 68.63 and 90.454 % hydrogen was generated at 25, 50, and 75 °C, respectively. From Figure 4.12, it can be seen that the hydrolysis rate increases significantly when the temperature increases. It can also be noticed that the oxalic acid solution shows faster hydrogen generation when compared to acetic and citric acid.

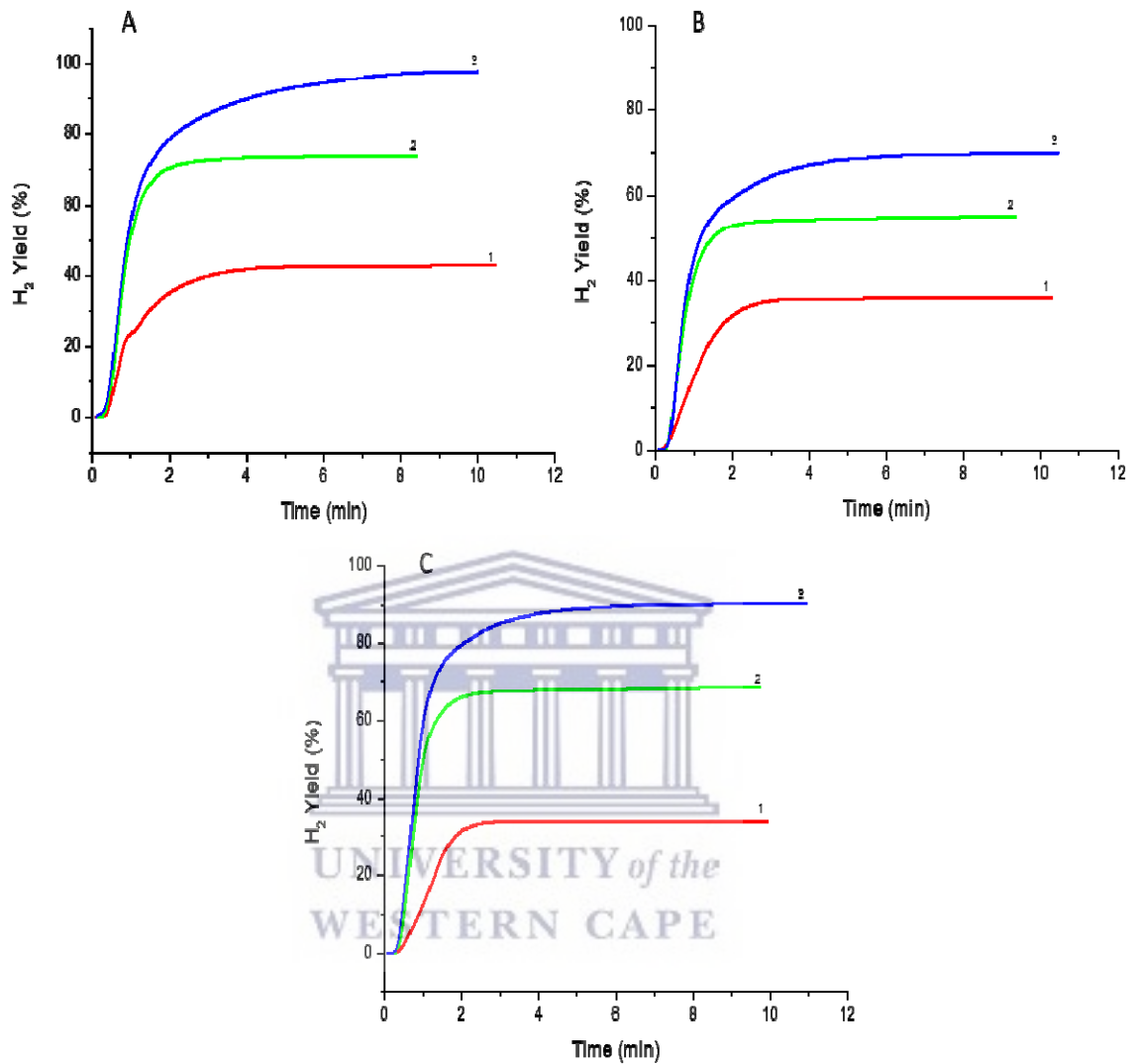


**Figure 4.13:** The hydrolysis of  $MgH_2$  (A) 1wt.% acetic acid at 25, 50 and 75 °C, (B) 1wt.% citric acid at 25, 50 and 75 °C, (C) 1wt.% oxalic acid at 25, 50 and 75 °C, where 1, 2 and 3 is 25 °C, 50 °C and 75 °C respectively.

#### 4.5. Activation energy of $MgH_2$ Hydrolysis in acetic, citric and oxalic acid

The Effect of reaction temperature on the rate of hydrogen generation was significant, as shown in Figure 4.13. Clearly, the increase in temperature increased the total hydrogen yield and hydrolysis rate. The relationship between

temperature and rate of hydrogen generation can generally be expressed by the Arrhenius equation.

$$\ln k = \ln A - E_a / RT \quad 4.6$$

where  $k$  is the reaction rate,  $E_a$  is the activation energy (J/mol),  $R$  is the universal gas constant (8.314 J/(mol.K)) and  $T$  is the temperature (K). Thus,  $E_a$  for  $MgH_2$  hydrolysis in different organic acids may be determined from Eq 4.6. Figure 4.14 shows the Arrhenius plots for  $MgH_2$  Hydrolysis in 1 wt. % acetic acid, 1 wt.% citric acid and 1 wt. % oxalic acid solutions. The  $r$ -value for  $MgH_2$  hydrolysis in acetic acid is 0.982, citric acid 0.986 and oxalic acid 0.992, indicating that the Arrhenius equation is appropriate for describing the hydrolysis. The apparent activation energies of  $MgH_2$  hydrolysis in 1 wt. % acetic acid, 1 wt. % citric acid and 1 wt.% oxalic acid solutions were 23.53 kJ/mol, 21.62 kJ/mol and 12.70 kJ/mol, respectively. Compared with the 58.06 kJ/mol in de-ionized water reported in the literature [76]. Thus, the addition of organic acids significantly lowers the  $E_a$  for  $MgH_2$  hydrolysis. A lower  $E_a$  value generally indicates higher reactivity. Therefore, the presence of organic acids enhances the hydrolysis properties of  $MgH_2$ .

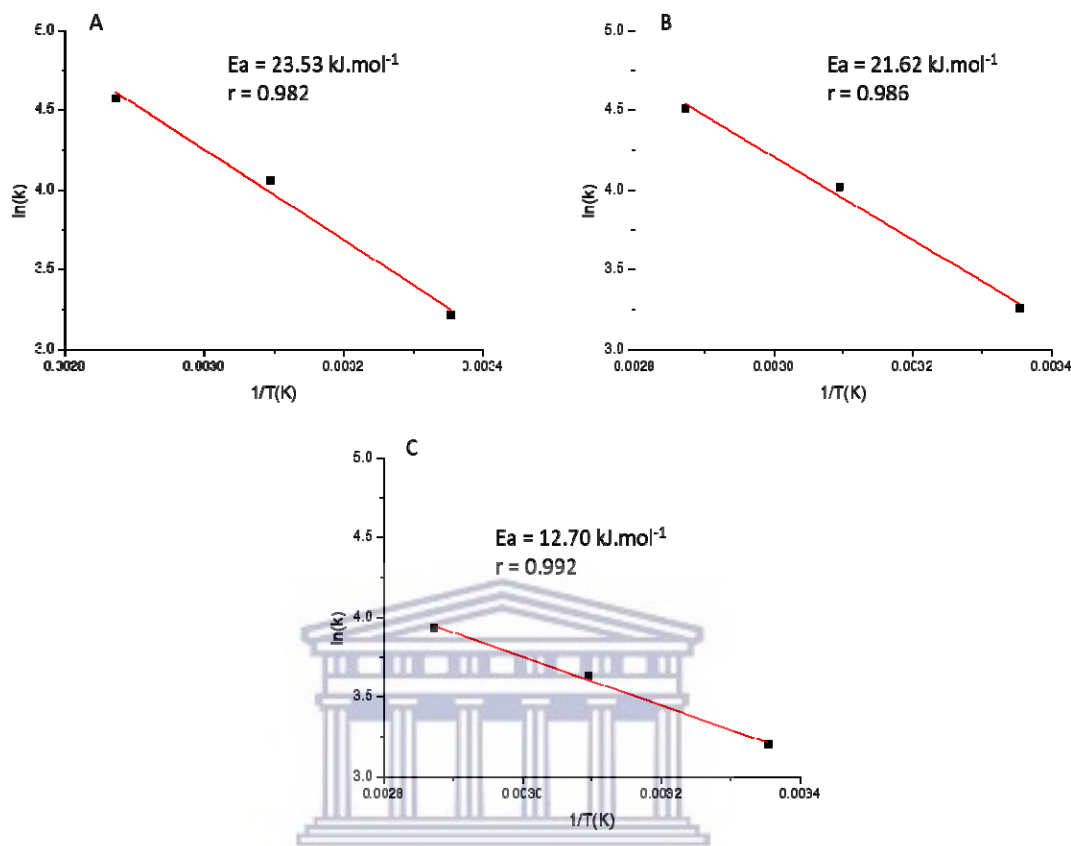


**Figure 4.14:** Arrhenius plots for the activation energy for the hydrogen generation in the Hydrolysis of  $MgH_2$  (A)  $MgH_2$  hydrolysis in 1 wt. % acetic acid solution, (B)  $MgH_2$  Hydrolysis in 1 wt. % citric acid solution, (c)  $MgH_2$  hydrolysis in 1 wt. % oxalic acid solution

#### 4.6 Effect of $AlCl_3$ on the hydrolysis of $MgH_2$

Chloride salts are potential catalytic materials in hydrolysis of  $MgH_2$ . Zhao et al. [77] claimed that  $MgCl_2$  efficiently catalyzed the hydrolysis of  $MgH_2$  showing that 96 % yield of hydrogen conversion was reached in 30 min at 303 K. Huang et al. [78] also found that the addition of  $NH_4Cl$  could effectively improve the hydrolysis kinetics of  $MgH_2$  and 1660 mL/g hydrogen can be produced in 30 min at 333 K by  $MgH_2$ -4.5 wt%  $NH_4Cl$  system. In this, study the possibility to enhance the hydrolysis performance of  $MgH_2$  was investigated by using  $AlCl_3$  solution as the

reaction medium. The hydrolysis properties of  $\text{MgH}_2$  and  $\text{AlCl}_3$  solutions with different concentrations have been investigated systematically. Figure 4.15, shows the kinetics of hydrogen generation by reacting  $\text{MgH}_2$  with 0.1, 0.2, 0.5 and 1 M  $\text{AlCl}_3$  solution at 25 °C. As shown in Figure 4.14, when the concentration of the  $\text{AlCl}_3$  solution increases the  $\text{H}_2$  yield also increase. The yield for hydrogen generation for 0.1, 0.2, 0.5 and 1 M  $\text{AlCl}_3$  solutions were 42.23, 48.92, 74.09 and 96.71 %, respectively. It was reported by Liu et.al [79] that  $\text{H}^+$  produced by the  $\text{Al}^{3+}$  hydrolysis can dissolve the  $\text{Mg}(\text{OH})_2$  passive layer, effectively. What's more  $\text{Cl}^-$  also causes the destruction of the  $\text{Mg}(\text{OH})_2$  film by pit corrosion process [80]. Table 4.8 shows the concentrations of the  $\text{AlCl}_3$  solution before and after hydrolysis. It can be seen that as the concentration of the  $\text{AlCl}_3$  solution increases the solutions become more acidic, this is due to more  $\text{H}^+$  ions produced by the  $\text{Al}^{3+}$  ions. This increase in  $\text{H}^+$  in the solution facilitates the destruction of the  $\text{Mg}(\text{OH})_2$  passive layer and thus promote the hydrolysis of  $\text{MgH}_2$  completely.

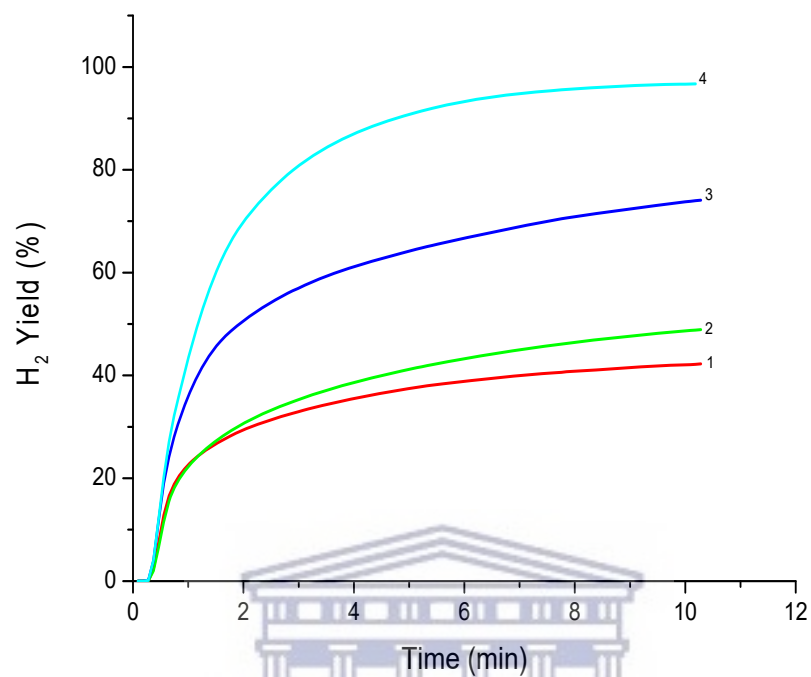


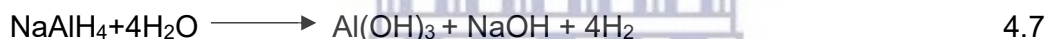
**Figure 4.15:** hydrolysis of  $MgH_2$  in  $AlCl_3$  solutions (1) 0.1 M  $AlCl_3$  solution, (2) 0.2 M  $AlCl_3$  solution, (3) 0.5 M  $AlCl_3$  solution, and (4) 1 M  $AlCl_3$  solution.

**Table 4.8:** pH of  $AlCl_3$  solutions at different concentrations before and after hydrolysis of  $MgH_2$  at 25°C

	$AlCl_3$ Solutions			
Concentration	0.1 M	0.2 M	0.5 M	1 M
Before hydrolysis	3.07	3.00	2.28	1.65
After hydrolysis	3.96	3.60	3.35	2.68

#### 4.7. Hydrolysis of Sodium Aluminium Hydride (NaAlH<sub>4</sub>)

Metal alanates such as LiAlH<sub>4</sub> and NaAlH<sub>4</sub> are another promising group of lightweight metals with high hydrogen content. These materials have been shown to be encouraging for hydrolysis reaction in water for hydrogen generation. The advantages of metal alanates for hydrolysis is that the reaction occurs at ambient temperature, no catalysts or acidic conditions are required, no insoluble metaborate by-products are formed and they are relatively cheap, however, one of the main disadvantages is that the hydrolysis reactions are very exothermic. The chemical equation for the reaction of NaAlH<sub>4</sub> with water is shown in Figure 4.7.



In this, study NaAlH<sub>4</sub> was used as a substrate to generate hydrogen via hydrolysis in water 200 mg of NaAlH<sub>4</sub> was reacted with 40 ml of water at 25 °C. Figure 4.16 shows the hydrolysis results for NaAlH<sub>4</sub> in water at 25 °C. From Figure 4.16 (A) it can be seen that the reaction is highly exothermic as there is an immediate increase in temperature of the reaction solution once NaAlH<sub>4</sub> is added as well as a sharp increase in hydrogen flow rate due to hydrogen generation. Figure 4.16 (B) show the kinetics of hydrogen generation in % yield, which can be seen that 90 % H<sub>2</sub> yield was achieved in less than 1 minute and the total H<sub>2</sub> yield after 15 minutes is 92.41%. Table 4.9 shows the pH of the reaction solution before and after hydrolysis. It can be seen that during hydrolysis, the reaction solution becomes basic, which is expected as from equation 4.7 Al(OH)<sub>3</sub> and NaOH are produced during hydrolysis of NaAlH<sub>4</sub>. This result shows that the hydrolysis of NaAlH<sub>4</sub> does not require acidic conditions to generate H<sub>2</sub>.



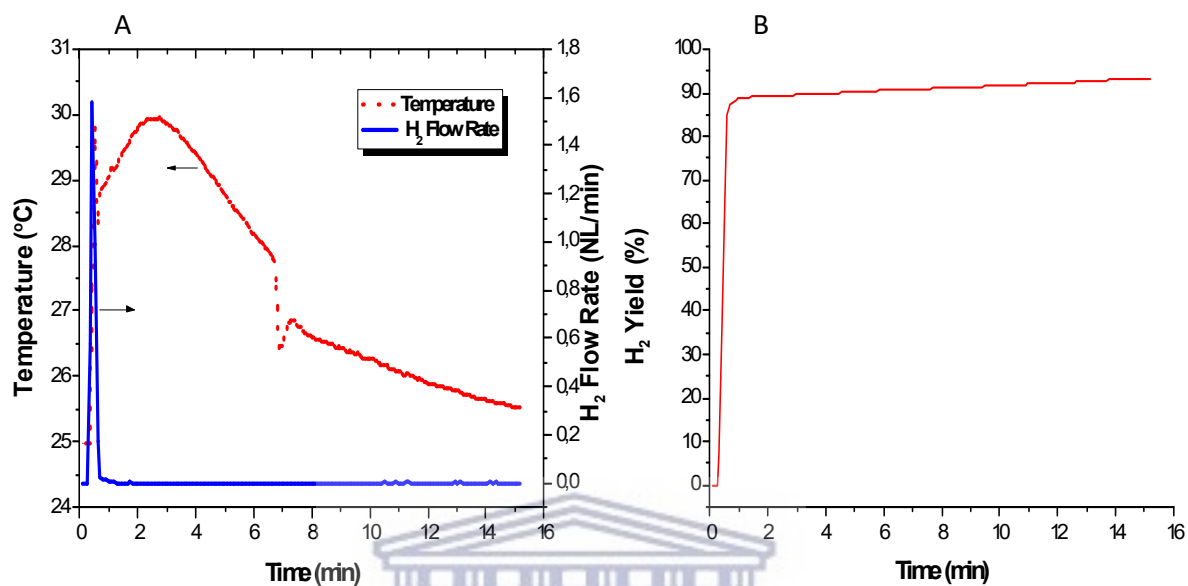


**Figure 4.16:** Hydrolysis of NaAlH<sub>4</sub> in water at 25 °C, (A) reaction solution temperature and H<sub>2</sub> flow rate during hydrolysis, (B) kinetics of H<sub>2</sub> generation.

**Table 4.9:** pH of reaction solution for NaAlH<sub>4</sub> before and after hydrolysis

NaAlH <sub>4</sub> in water at 25°C	
pH Before hydrolysis	7.89
pH After hydrolysis	11.60

---

## Conclusions and Recommendations

This chapter presents the conclusions and recommendations of the study. The main objective of the present study was to improve the hydrolysis of  $\text{MgH}_2$  for hydrogen generation. The main challenge with using  $\text{MgH}_2$  for hydrolysis as a hydrogen generation material is slow reaction kinetics due to the formation of the  $\text{Mg}(\text{OH})_2$  passivation layer, which hinders hydrogen generation. In the current research study, the ball milling of  $\text{MgH}_2$  and the addition of various organic acids and aluminium chloride to the reaction solution was undertaken. Based on the results obtained in the current work, the results are summarized below as follows.

### 5.1. Conclusions

The research study reports on the improvement in hydrogen generation of  $\text{MgH}_2$  through various interventions such as increasing temperature, ball milling, improving reaction kinetics through application of organic acids such as (acetic, citric and oxalic acids) and the addition of aluminium chloride.

- The increase in temperature of the hydrolysis reaction solution (25, 50 and 75 °C) leads to an increase in reaction rates and hydrogen yields. However, the  $\text{H}_2$  yield is still relatively low due to the formation of the  $\text{Mg}(\text{OH})_2$  passivation layer on the surface of the substrate.
- The effect of ball milling  $\text{MgH}_2$  has been shown to increase the yield of  $\text{H}_2$  generation by hydrolysis compared to the as-received  $\text{MgH}_2$ . The increase in  $\text{H}_2$  yield can mainly be attributed to an increase in specific surface area. However, the  $\text{H}_2$  yield was still relatively low, which was also due to the formation of the  $\text{Mg}(\text{OH})_2$  passivation layer.

- The effect of organic acids such as acetic, citric and oxalic acid on the hydrolysis of  $MgH_2$  at various concentrations on hydrogen generation was evaluated experimentally. The hydrogen generation was considerably improved by using organic acid solution instead of only deionized water due to the organic acid dissolving the  $Mg(OH)_2$  passivation layer.
- The addition of organic acids to the hydrolysis solution caused the solution to be acidic. Therefore, during hydrolysis of  $MgH_2$  in the acidic solution causes less  $OH^-$  to be released into the solution and, in turn, limits the formation of the  $Mg(OH)_2$  passivation layer.
- $AlCl_3$  has been shown to be an effective additive for the hydrolysis of  $MgH_2$ . The results have shown that as we increase the concentration of the  $AlCl_3$  solution, the reaction kinetics and the yield of  $H_2$  increase. This was due to the reaction solution becoming acidic due to  $Al^{3+}$  producing  $H^+$  ions which also consumes the  $Mg(OH)_2$ .
- The hydrolysis of  $NaAlH_4$  was shown to generate  $H_2$  at ambient temperature without the addition of acids or catalysts. The  $H_2$  yield was relatively high, with 90 %  $H_2$  produced in one minute however, the reaction is very exothermic in nature.

## 5.2 Recommendation

Based in the analyses and conclusions of the study, several recommendations regarding future research directions of the investigation were made:

- Efforts should be made to study the purity of the H<sub>2</sub> generation via hydrolysis of MgH<sub>2</sub>, especially in organic acids, to see what impurities are present, which will help prevent damage to the H<sub>2</sub> fuel cell.
- The study has shown that the AlCl<sub>3</sub> is an excellent additive for the hydrolysis of MgH<sub>2</sub>; in the future, the research focus should extend to other chlorides such as MgCl<sub>2</sub> and NaCl<sub>2</sub> to see the effect on the hydrolysis of MgH<sub>2</sub>.
- Design of the reactors capable of producing hydrogen via hydrolysis at higher pressure than most glass vessels currently reported in the literature that cannot withstand high pressure from the exothermic reactions of metal hydride hydrolysis.

---

## REFERENCES

### References:

- [1] M. D. Leonard, E. E. Michaelides, and D. N. Michaelides, "Energy storage needs for the substitution of fossil fuel power plants with renewables," *Renew. Energy*, vol. 145, pp. 951–962, Jan. 2020.
- [2] S. Z. Baykara, "Hydrogen: A brief overview on its sources, production and environmental impact," *Int. J. Hydrogen Energy*, vol. 43, no. 23, pp. 10605–10614, 2018.
- [3] J. A. Adeniran, E. T. Akinlabi, H. S. Chen, R. Fono-Tamo, and T. C. Jen, "Organic acid-catalyzed hydrolysis of magnesium hydride for generation of hydrogen in a batch system hydrogen reactor," *Lect. Notes Eng. Comput. Sci.*, vol. 2, pp. 615–619, 2017.
- [4] Z. Wang and G. F. Naterer, "ScienceDirect Integrated fossil fuel and solar thermal systems for hydrogen production and CO<sub>2</sub> mitigation," *Int. J. Hydrogen Energy*, vol. 39, no. 26, pp. 14227–14233, 2014.
- [5] P. Thungklin, S. Sittijunda, and A. Reungsang, "ScienceDirect Sequential fermentation of hydrogen and methane from steam-exploded sugarcane bagasse hydrolysate," *Int. J. Hydrogen Energy*, vol. 43, no. 21, pp. 9924–9934, 2018.
- [6] H. J. Yun, H. Lee, J. B. Joo, N. D. Kim, and J. Yi, "Effect of TiO<sub>2</sub> Nanoparticle Shape on Hydrogen Evolution via Water Splitting," vol. 11, no. xx, pp. 1–4, 2011.
- [7] M. Mostajeran, V. Prévot, S. S. Mal, E. Mattiussi, B. R. Davis, and R. T. Baker, "Base-metal catalysts based on porous layered double hydroxides for

alkaline-free sodium borohydride hydrolysis," *Int. J. Hydrogen Energy*, vol. 42, no. 31, pp. 20092–20102, 2017.

[8] D. Rohendi, N. Syarif, and E. K. Wati, "Storage and Release of Hydrogen as a Fuel of the Fuel Cell with Media of NaBO<sub>2</sub>/NaBH<sub>4</sub>," *IOP Conf. Ser. Earth Environ. Sci.*, vol. 248, no. 1, 2019.

[9] P. Brack, S. E. Dann, and K. G. Upul Wijayantha, "Heterogeneous and homogenous catalysts for hydrogen generation by hydrolysis of aqueous sodium borohydride (NaBH<sub>4</sub>) solutions," *Energy Sci. Eng.*, vol. 3, no. 3, pp. 174–188, 2015.

[10] H. Zhong *et al.*, "Enhanced hydrolysis properties and energy efficiency of MgH<sub>2</sub>-base hydrides," *J. Alloys Compd.*, vol. 680, pp. 419–426, 2016.

[11] M. Ma, L. Ouyang, J. Liu, H. Wang, and H. Shao, "Air-stable hydrogen generation materials and enhanced hydrolysis performance of MgH<sub>2</sub>-LiNH<sub>2</sub> composites," vol. 359, 2017.

[12] B. Kieback, R. Lars, M. Tegel, and S. Sch, "ScienceDirect An efficient hydrolysis of MgH<sub>2</sub>-based materials," vol. 2, 2016.

[13] A. M. Abdalla, S. Hossain, O. B. Nisfindy, A. T. Azad, M. Dawood, and A. K. Azad, "Hydrogen production, storage, transportation and key challenges with applications: A review," *Energy Convers. Manag.*, vol. 165, no. April, pp. 602–627, 2018.

[14] C. Acar and I. Dincer, "Comparative assessment of hydrogen production methods from renewable and non-renewable sources," *Int. J. Hydrogen Energy*, vol. 39, no. 1, pp. 1–12, 2014.

[15] N. Abas, A. Kalair, and N. Khan, "Review of fossil fuels and future energy technologies," *Futures*, vol. 69, pp. 31–49, 2015.

- [16] M. Höök and X. Tang, "Depletion of fossil fuels and anthropogenic climate change-A review," *Energy Policy*, vol. 52, no. April 2018, pp. 797–809, 2013.
- [17] S. Sorrell, "Reducing energy demand: A review of issues, challenges and approaches," *Renew. Sustain. Energy Rev.*, vol. 47, pp. 74–82, 2015.
- [18] P. A. Owusu and S. Asumadu-sarkodie, "CIVIL & ENVIRONMENTAL ENGINEERING | REVIEW ARTICLE A review of renewable energy sources , sustainability issues and climate change mitigation," *Cogent Eng.*, vol. 15, no. 1, pp. 1–14, 2016.
- [19] A. Mohamed and M. T. Khan, "A review of electrical energy management techniques : supply and consumer side ( industries )," vol. 20, no. 3, 2009.
- [20] K. Mazloomi and C. Gomes, "Hydrogen as an energy carrier: Prospects and challenges," *Renew. Sustain. Energy Rev.*, vol. 16, no. 5, pp. 3024–3033, 2012.
- [21] M. Helen McCay, "Hydrogen. An Energy Carrier.," *Futur. Energy Improv. Sustain. Clean Options our Planet*, no. April, pp. 495–510, 2013.
- [22] M. A. Rosen and S. Koochi-Fayegh, "The prospects for hydrogen as an energy carrier: an overview of hydrogen energy and hydrogen energy systems," *Energy, Ecol. Environ.*, vol. 1, no. 1, pp. 10–29, 2016.
- [23] S. Sharma and S. K. Ghoshal, "Hydrogen the future transportation fuel: From production to applications," *Renew. Sustain. Energy Rev.*, vol. 43, pp. 1151–1158, 2015.
- [24] J. O. Abe, A. P. I. Popoola, E. Ajenifuja, and O. M. Popoola, "Hydrogen energy, economy and storage: Review and recommendation," *Int. J. Hydrogen Energy*, vol. 44, no. 29, pp. 15072–15086, 2019.
25. Yartys V.A., Lototsky M.V. An overview of hydrogen storage methods, *Hydrogen Materials Science and Chemistry of Carbon Nanomaterials*, ed. by T.

Nejat Veziroglu, Svetlana Yu. Zaginaichenko, Dmitry V. Schur, B. Baranowski, Anatoliy P. Shpak, and Valeriy V. Skorokhod. – Kluwer Academic Publishers, 2004, pp. 75-104

26. Rivard E., Trudeau M., Zaghbi K. Hydrogen storage for mobility: A review, *Materials* 12(12) (2019)1973. DOI:10.3390/ma12121973

27. Zacharia R., Rather S.U. Review of solid state hydrogen storage methods adopting different kinds of novel materials, *Journal of Nanomaterials* 2015, 914845. DOI: 10.1155/2015/914845

28. L. Ouyang, F. Liu, H. Wang, J. Liu, X.-S. Yang, L. Sun, M. Zhu. Magnesium-based hydrogen storage compounds: A review, *Journal of Alloys and Compounds* 832 (2020) 154865. DOI: 10.1016/j.jallcom.2020.154865

29. Aziz M., TriWijayanta A., Nandiyanto A.B.D. Ammonia as effective hydrogen storage: A review on production, storage and utilization, *Energies* 13(12) (2020) en13123062. DOI:10.3390/en13123062

30. Hassan I.A., Ramadan H.S., Saleh M.A., Hissel D. Hydrogen storage technologies for stationary and mobile applications: Review, analysis and perspectives, *Renewable and Sustainable Energy Reviews* 149 (2021)111311. DOI: 10.1016/j.rser.2021.111311

[31] R. Moradi and K. M. Groth, “Hydrogen storage and delivery: Review of the state of the art technologies and risk and reliability analysis,” *Int. J. Hydrogen Energy*, vol. 44, no. 23, pp. 12254–12269, 2019.

[32] B. Sørensen, G. Spazzafumo. 2 – Hydrogen, in: *Hydrogen and Fuel Cells* (Third Edition), Elsevier, 2018. <https://doi.org/10.1016/B978-0-08-100708-2.0002-3>



- [33] D. Teichmann, W. Arlt, and P. Wasserscheid, "Liquid Organic Hydrogen Carriers as an efficient vector for the transport and storage of renewable energy," *Int. J. Hydrogen Energy*, vol. 37, no. 23, pp. 18118–18132, 2012.
- [34] A. Gonza, E. Soria, J. Dufour, and D. P. Serrano, "Life cycle assessment of alternatives for hydrogen production from renewable and fossil sources," vol. 7, 2011.
- [35] I. Dincer and C. Zamfirescu, "Sustainable hydrogen production options and the role of IAHE," *Int. J. Hydrogen Energy*, vol. 37, no. 21, pp. 16266–16286, 2012.
- [36] F. Suleman and I. Dincer, "ScienceDirect Environmental impact assessment and comparison of some hydrogen production options," *Int. J. Hydrogen Energy*, vol. 40, no. 21, pp. 6976–6987, 2015.
- [37] A. Miltner, W. Wukovits, T. Pröll, and A. Friedl, "Renewable hydrogen production : a technical evaluation based on process simulation," *J. Clean. Prod.*, vol. 18, pp. S51–S62, 2010.
- [38] K. Mazloomi and C. Gomes, "Hydrogen as an energy carrier : Prospects and challenges," *Renew. Sustain. Energy Rev.*, vol. 16, no. 5, pp. 3024–3033, 2012.
- [39] M. F. Orhan, I. Dincer, M. A. Rosen, and M. Kanoglu, "Integrated hydrogen production options based on renewable and nuclear energy sources," *Renew. Sustain. Energy Rev.*, vol. 16, no. 8, pp. 6059–6082, 2012.
- [40] H.K. Jua, S. Badwalb, S. Giddey, A comprehensive review of carbon and hydrocarbon assisted water electrolysis for hydrogen production, *Appl. Energy*, 231 (2018), pp. 502-533

- [41] P. Nikolaidis, A. Poullikkas, A comparative overview of hydrogen production processes, *Renewable Sustainable Energy Rev.*, 67 (2017), pp. 597-611
- [42] S.A. Grigoriev, V.I. Poremsky, V.N. Fateev, Pure hydrogen production by PEM electrolysis for hydrogen energy, *Int. J. Hydrogen Energy*, 31 (2006), pp. 171-175
- [43] P. Millet, R. Ngameni, S.A. Grigoriev, N. Mbemba, F. Brisset, A. Ranjbari, et al. PEM water electrolyzers: from electrocatalysis to stack development, *Int. J. Hydrogen Energy*, 35 (2010), pp. 5043-5052
- [44] L. D. Souza, "Thermochemical hydrogen production from water using reducible oxide materials : a critical review," 2013.
- [45] C. B. Porciúncula, N. R. Marcilio, I. C. Tessaro, and M. Gerchmann, "PRODUCTION OF HYDROGEN IN THE REACTION BETWEEN ALUMINUM AND WATER IN THE PRESENCE OF NaOH AND KOH," vol. 29, no. 02, pp. 337–348, 2012.
- [46] J. Petrovic, G. Thomas, "Reaction of Aluminum with Water to Produce Hydrogen," U.S. Department of Energy pp. 1–26, 2008.
- [47] K. Mahmoodi and B. Alinejad, "Enhancement of hydrogen generation rate in reaction of aluminum with water," *Int. J. Hydrogen Energy*, vol. 35, no. 11, pp. 5227–5232, 2010.
- [48] S. Elitzur, V. Rosenband, and A. Gany, "ScienceDirect Study of hydrogen production and storage based on aluminum e water reaction," *Int. J. Hydrogen Energy*, vol. 39, no. 12, pp. 6328–6334, 2014.
- [49] S.C. Amendola, S.L. Sharp-Goldman, M.S. Janjua, M.T. Kelly, P.J. Petillo, M. Binder, An ultrasafe hydrogen generator: aqueous, alkaline borohydride solutions and Ru catalyst, *J. Power Sources* 85 (2000) 186e189.

- [50] Şahin, Ö., D. Kılınç, and C. Saka, Hydrogen generation from hydrolysis of sodium borohydride with a novel palladium metal complex catalyst. *Journal of the Energy Institute*, 2016. 89(2): p. 182-189.
- [51] Amendola, S.C., et al., A safe, portable, hydrogen gas generator using aqueous borohydride solution and Ru catalyst. *International Journal of Hydrogen Energy*, 2000. 25(10): p. 969-975.
- [52] T. Hiraki, S. Hiroi, T. Akashi, and N. Okinaka, "Chemical equilibrium analysis for hydrolysis of magnesium hydride to generate hydrogen," *Int. J. Hydrogen Energy*, vol. 37, no. 17, pp. 12114–12119, 2012.
- [53] S. D. Kushch, N. S. Kuyunko, R. S. Nazarov, and B. P. Tarasov, "Hydrogen-generating compositions based on magnesium," *Int. J. Hydrogen Energy*, vol. 36, no. 1, pp. 1321–1325, 2010.
- [54] M. Huang, L. Ouyang, H. Wang, J. Liu, and M. Zhu, "Hydrogen generation by hydrolysis of MgH<sub>2</sub> and enhanced kinetics performance of ammonium chloride introducing," *Int. J. Hydrogen Energy*, vol. 40, no. 18, pp. 6145–6150, 2015.
- [55] C. J. Webb, "Journal of Physics and Chemistry of Solids A review of catalyst-enhanced magnesium hydride as a hydrogen storage material," *J. Phys. Chem. Solids*, vol. 84, pp. 96–106, 2015.
- [56] X. Xie *et al.*, "Recent advances in hydrogen generation process via hydrolysis of Mg- based materials : A short review," *J. Alloys Compd.*, vol. 816, p. 152634, 2020.
- [57] K. Wang, G. Wu, H. Cao, and H. Li, "ScienceDirect Improved reversible dehydrogenation properties of MgH<sub>2</sub> by the synergetic effects of graphene oxide-based porous carbon and TiCl<sub>3</sub>," *Int. J. Hydrogen Energy*, vol. 43, no. 15, pp. 7440–7446, 2018.

- [58] L. G. Sevastyanova, S. N. Klyamkin, and B. M. Bulychev, "ScienceDirect Generation of hydrogen from magnesium hydride oxidation in water in presence of halides," *Int. J. Hydrogen Energy*, vol. 45, no. 4, pp. 3046–3052, 2019.
- [59] M. Hirscher *et al.*, "Materials for hydrogen-based energy storage – past, recent progress and future outlook," *J. Alloys Compd.*, vol. 827, 2020.
- [60] I. E. Malka, T. Czujko, and J. Bystrzycki, "Catalytic effect of halide additives ball milled with magnesium hydride," *Int. J. Hydrogen Energy*, vol. 35, no. 4, pp. 1706–1712, 2010.
- [61] D. Gan, Y. Liu, J. Zhang, Y. Zhang, and C. Cao, "ScienceDirect Kinetic performance of hydrogen generation enhanced by  $\text{AlCl}_3$  via hydrolysis of  $\text{MgH}_2$  prepared by hydriding combustion synthesis," *Int. J. Hydrogen Energy*, vol. 43, no. 22, pp. 10232–10239, 2018.
62. V. Berezovets, A. Kytsya, I. Zavaliy, V. A. Yartys. Kinetics and mechanism of  $\text{MgH}_2$  hydrolysis in  $\text{MgCl}_2$  solutions, *Int. J. Hydrogen Energy* 46 (2021) 40278-40293
- [63] C. H. Chao and T. C. Jen, "Reaction of magnesium hydride with water to produce hydrogen," *Appl. Mech. Mater.*, vol. 302, no. February, pp. 151–157, 2013.
- [64] L. Ouyang *et al.*, "Enhanced hydrogen generation properties of  $\text{MgH}_2$ -based hydrides by breaking the magnesium hydroxide passivation layer," *Energies*, vol. 8, no. 5, pp. 4237–4252, 2015.
- [65] H. Uesugi, T. Sugiyama, H. Nii, T. Ito, and I. Nakatsugawa, "Industrial production of  $\text{MgH}_2$  and its application," pp. 650–653, 2011.
- [66] S. Li, D. Gan, Y. Zhu, Y. Liu, G. Zhang, and L. Li, "Influence of chloride salts on hydrogen generation via hydrolysis of  $\text{MgH}_2$  prepared by hydriding

combustion synthesis and mechanical milling,” *Trans. Nonferrous Met. Soc. China*, vol. 27, no. 3, pp. 562–568, 2017.

[67] W. Cao, “Synthesis of Nanomaterials by High Energy Ball Milling,” UnderstandingNano.com, 2007. [Online]. Available: <http://www.understandingnano.com/nanomaterial-synthesis-ball-milling.html>. [Accessed: 16-Jan-2017].

[68] C. Suryanarayana, “Mechanical alloying and milling,” *Prog. Mater. Sci.*, vol. 46, no. 1–2, pp. 1– 184, Jan. 2001.

[69] Varin, R.A., et al., Nanomaterials for hydrogen storage produced by ball milling. *Canadian Metallurgical Quarterly*, 2009. 48(1): p. 11-25.

[70] R.V. Denys, et al, *Acta Materialia* 57 (2009) 3989–4000

[71] Moriwaki T., Akahama Y., Kawamura H., Nakano S., Takemura K. Structural phase transition of rutile-type MgH<sub>2</sub> at high pressures, *J. Phys. Soc. Jpn.* (2006) 75, 074603-1

[72] Zavaliy I., Denys R.V., Berezovets V., Paul Boncour V. Phase relationships in the Mg-Ti-Ni system at 450°C, *Coll. Abs. 10th Int. Conf. Crystal Chem. Internet. Compd. (Lvov) 2007*, -58

[73] Feng Z., Babu V.S., Zhao J., Seehra M.S. Effect of magnetic dilution on magnetic ordering in Ni<sub>2</sub>Mg<sub>1-p</sub>O, *J. Appl. Phys.* (1991) 70, 6161-6163

[74] Webb, C.J., A review of catalyst-enhanced magnesium hydride as a hydrogen storage material. *Journal of Physics and Chemistry of Solids*, 2015. 84: p. 96-106.

[75] M.-H. Grosjean, M. Zidoune, L. Roue . Hydrogen production from highly corroding Mg-based materials elaborated by ball milling, *Journal of Alloys and Compounds* 404–406 (2005) 712–715

- [76] M.Huang, L.Ouyang, H. Wang, J.Liu, M.Zhu, Hydrogen generation by Hydrolysis of MgH<sub>2</sub> and enhanced kinetics performance of ammonium chloride introducing, International Journal of Hydrogen Energy, 40 (2015) 6145-6150.
- [77] Zhao ZL, Zhu YF, Li LQ. Efficient catalysis by MgCl<sub>2</sub> in hydrogen generation via hydrolysis of Mg-based hydride prepared by hydriding combustion synthesis. Chem Commun 2012; 48 (44): 5509-11.
- [78] Huang M, Ouyang L, Wang H, Liu JW, Zhu M, Hydrogen generation by hydrolysis of MgH<sub>2</sub> and enhanced kinetics performance of ammonium chloride introduction. Int. Journal of Hydrogen Energy 2015; 40 (18): 6145-6150
- [79] Liu YA, Wang XH, Dong ZH, Liu HZ, Li SQ, Ge HW; Hydrogen generation from Mg powder ball-milled with AlCl<sub>3</sub>; Energy, 2013; 53 (5):147-152
- [80] Tessier JP, Palau P, Huot J, Schulz R, Guay D. Hydrogen production and crystal structure of ball-milled MgH<sub>2</sub>-Ca and MgH<sub>2</sub>-CaH<sub>2</sub> mixtures, J Alloys and Compounds, 2004, 376 (1-2),180-185